Aalborg University

10th Semester

Mathematics-Economics

Master's Thesis

# Validation of a GMM Approach to Estimate Parameters in a Rough Volatility Setting in the Presence of Microstructure Noise

June 2, 2022

AALBORG UNIVERSITET
STUDENTERRAPPORT

**Fifth year w/**
**Department of Mathematical Sciences**
Mathematics-Economics
Skjernvej 4A
9220 Aalborg Ø
http://www.studerende.math.aau.dk/

**Title:**

Validation of a GMM Approach to Estimate Parameters in a Rough Volatility Setting in the Presence of Microstructure Noise

**Project period:**

1st of February 2022 - 3rd of June 2022

**Project group:**

math-22-matoek-10-1204b

**Participants:**

Asbjørn Bach

Asbjørn Bach Andreassen

Rasmus Dam

Rasmus Dam

**Supervisor:**
Orimar Sauri Arregui

**Abstract:**

This project seeks to validate a GMM approach to estimating parameters in a volatility process driven by a fractional Ornstein-Uhlenbeck process, in the presence of microstructure noise. To this end we have done a simulation study showing and validating microstructure noises effect on the GMM approach with different estimators of integrated volatility, namely classic realized volatility, realized volatility with 5 min sampling and modulated realized covariance, which is a microstructure noise robust estimator.
The result of the simulation study showed signs that the theoretical distribution of the parameters was unaffected by the presence of microstructure noise, when using a microstructure noise robust estimator for integrated volatility.
Lastly, we applied the GMM method on high-frequency price data for the S&P500 ETF SPY for the period 1999 to 2009 where we found that the volatility process was indeed rough, in line with other similar works.

**Page count: 38**

# Preface

The group would like to give a special thanks to:
- *Orimar Sauri Arregui, supervisor, for help, advice and guidance throughout the duration of the project.*

The group has used the following programs in the writing of this report

- **Overleaf** - Writing.
- **Google drive** - Notes and file sharing.
- **R** - Statistical calculations and data analysis.
- **Github** - Version control.

**Reader's Guide:**

On page v, a table of contents is given. When viewing this report as a PDF, hyperlinks in the table of content will allow fast navigation to the desired section.

The bibliography on page 38 presents the literature used in this report. The references are given in the following format:

[Author][Title](Institution)(ISBN)[Year](URL)(Date Accessed)

Where fields in [square brackets] are mandatory, while regular parenthesis only are relevant for certain formats (e.g. books or web pages). The bibliography entries are sorted after the appearance in the text.

# Contents

## Chapter 1

# Introduction

The underlying generating process of asset prices has been of interest for decades, and being able to model it effectively has been something to strive for. The assumptions of the generating process has changed through time. The generating process was viewed as a time series with ARCH and GARCH variations, it has been viewed as a stochastic process starting with random walks, which slowly evolved into more complicated setups. Black and Scholes had a breakthrough in the seventies, stemming from the release of "The Pricing of Options and Corporate Liabilities" [Black and Scholes, 1973]. The issue with the Black and Scholes model was however that volatility was assumed constant, this assumption is violated by the empirically estimated volatility smile. In the Dupire local volatility model [Dupire et al., 1994], the local volatility is a deterministic function of the underlying price and time, chosen to match observed European option prices. This model has highly unrealistic dynamics and create future volatility surfaces unlike those observed. Other models allowed for stochastic volatility, e.g. the Heston model where the volatility process was a markovian process. Whilst stochastic volatility dynamics are more realistic than local volatility dynamics, generated option prices from these types of models are not consistent with observed European option prices. Furthermore, the stochastic volatility models do not fit the volatility surface [Gatheral et al., 2018]. In particular, At the-money ($k = 0$) volatility skew

$$\psi(p) := \left| \frac{\partial}{\partial p} \sigma_{BS}(k, p) \right|,$$

is well approximated by a power law function of time to expiry $p$. In contrast, conventional stochastic volatility models generate a term structure of at-the-money skew that is constant for small $p$ and behaves as a sum of decaying exponentials for larger $p$. In the paper [Fukasawa, 2011], they used a stochastic volatility model where the volatility is driven by a fractional Brownian motion with Hurst index $H$. This model generated an ATM skew of the form, $\psi(p) = p^{H-\frac{1}{2}}$ at least for small $p$. This provided a counterexample to the widespread belief that the explosion of the volatility smile as $p \to 0$ implies the presence of jumps. In order to generate volatility surfaces with a reasonable shape, $H$ had to be close to zero [Gatheral et al., 2018]. In the paper [Gatheral et al., 2018], they estimated smoothness of the volatility process by investigating the moments of the increments of log-volatility.

$$\mathbb{E}[|log(\sigma_\Delta) - log(\sigma_0)|^q] = b_q \Delta^{\zeta_q},$$

where $\Delta$ is a mesh. Plotting $\zeta_q$ against $q$, they obtained that $\zeta_q \sim Hq$, and found that empirically $H$ was indeed quite small. These findings do however rely on an estimation of the spot volatility, which is noisy and inaccurate.

When the volatility process is driven by a fractional Brownian motion with Hurst index smaller than 0.5 it is called a rough volatility model. This is the new generation of underlying price generation process dubbed by Jim Gatheral, Thibault Jaisson and Mathieu Rosenbaum. Rough is referring to short-memory and erratic nature. Historically, it has nearly been accepted as a stylized fact that volatility had long-memory properties, however [Gatheral et al., 2018] found that a rough fractional volatility model, where the volatility process is driven by a fractional Ornstein-Uhlenbeck process, was remarkably consistent with volatility time series data. The rough fractional volatility model they used did not have any long memory properties, and outperformed conventional AR and HAR volatility forecasts. Which motivates the use of rough volatility models when striving towards describing the price process effectively.

Rough volatility violates the typical log-price process setup, where the volatility process is assumed to be a semi-martingale. This somewhat invalidates the empirical findings obtained using the typical setup, if volatility truly is rough.

In this project, we seek to describe the underlying price generating process with a rough volatility setup, the chosen model has parameters, which we would like to estimate.

Estimating parameters in the model can be done in multiple ways, for example generalized method of moments (GMM), likelihood approaches or machine learning. In this project, the method of choice will be GMM. In [Bolko, 2021], they are using a GMM approach to estimate parameters in the process driving spot volatility, the process being a Fractional Ornstein-Uhlenbeck process. They used realized volatility as estimator for integrated volatility with 5 minute observations, RV5, as to not be affected by potential microstructure noise, and thereby obtain an estimate of $H$ with estimates of integrated variance instead of estimates of spot volatility like in [Gatheral et al., 2018], which should reduce the amount of noise included in the estimation of $H$. In this project, we want to take a similar approach, however we would not like to neglect a huge number of observations, and instead we would rely on a high frequency setting, from which we need to deal with microstructure noise. Realized volatility is not a microstructure robust estimator, which will be needed for this setting. For this purpose, we will be using the modulated realized covariance estimator, MRC, described in [Christensen et al., 2010].

With a model at hand, a way of estimating the parameters and a microstructure noise robust estimator for integrated volatility. We would like to validate the GMM approach through a simulation study, as well as compare the estimation procedure and parameter distribution using both MRC and RV5 as estimators for integrated volatility. Finally, we will apply the GMM procedure to high frequency prices for the S&P500 ETF SPY to estimate the parameters and potential roughness.

**Outline of Chapters**

In Chapter 2, the semi-martingale price model is presented along with the volatility process and the driver of the volatility process, which for this project is a fractional Ornstein-Uhlenbeck process. This is followed by a presentation of the generalized method of moments estimation procedure along with asymptotic properties of the estimated parameters. Lastly, the assumptions on microstructure noise are introduced, with its effect on estimation of integrated volatility.

In Chapter 3 the model for simulation is presented along with the models parameter specification, initial guesses, optimization procedure and two methods of validating the distribution of the parameters. This is followed by Tables illustrating the accuracy of the estimation procedure, both when microstructure noise is present and when it is not, and for different estimators of integrated volatility. Lastly, graphs are shown to validate the distribution of the parameters in a finite setting.

In Chapter 4, we apply the estimation procedure to S&P 500 and present the results.

In Chapter 5, we discuss the decisions made throughout the project along with potential different tweaks and their effect on the estimation. Lastly, we conclude on the results obtained.

Chapter 2

# Theory

## 2.1 The Semi-martingale Price Process

Firstly, assumptions about the behavior of the log-price as well as assumptions about the volatility process are needed.

This section is based on [Bolko, 2021].

Throughout the project, the log-price of a financial asset, $X = (X_\tau)_{\tau\geq 0}$ will be modeled by an adapted continuous-time stochastic process on a filtered probability space $(\Omega, \mathscr{F}, (\mathscr{F}_\tau)_{\tau\geq 0}, \mathbb{P})$. A standard arbitrage free market is assumed where asset log-prices are of semi-martingale form, i.e. $X$ can be described by the itô process

$$X_\tau = X_0 + \int_0^\tau \mu_s ds + \int_0^\tau \sigma_s dW_s, \quad \tau \geq 0, \tag{2.1}$$

where $X_0$ is $\mathscr{F}_0$-measurable, $\mu = (\mu_\tau)_{\tau\geq 0}$ is a predictable drift process, $\sigma = (\sigma_\tau)_{\tau\geq 0}$ is a càdlàg volatility process and $W = (W_\tau)_{\tau\geq 0}$ is a standard Brownian motion.

This setup differs from the typical semi-martingale setup, since neither the volatility process nor the log volatility process is necessarily a semi-martingale.

For the spot volatility we will assume a model as to incorporate rough volatility, we model $\sigma^2 = (\sigma_\tau^2)_{\tau\geq 0}$ as

$$\sigma_\tau^2 = \xi \exp\left(Y_\tau - \frac{1}{2}\kappa(0)\right), \quad \tau \geq 0, \tag{2.2}$$

with $\xi \in (0, \infty)$, a scale parameter representing the unconditional mean of the stochastic volatility, the process $Y = (Y_\tau)_{\tau\geq 0}$ is a zero-mean stationary Gaussian process with covariance function $\kappa(u) = cov(Y_0, Y_u) = \kappa_\phi(u), u \geq 0$, parameterized by $\phi \in \mathbb{R}^p$, where $p$ is going to depend on the chosen model for $Y$, denote $\theta = (\xi, \phi)$.

For estimation of the parameters of the model, we will use the integrated volatility for day $t$ defined as

$$IV_t = \int_{t-1}^t \sigma_s^2 ds, \quad t \in \mathbb{N},$$

which holds information on the model. This can be estimated by realized volatility or a microstructure noise-robust estimator if microstructure noise is present. The presence of Microstructure noise will be expanded upon in a section later.

### 2.1.1 Properties of Integrated Volatility

In this section, we will present some properties of Integrated Volatility under (2.1) and (2.2). This will serve as a foundation for the GMM approach, which will be presented in a section later.

**Theorem 1**

*Suppose that* (2.1) *and* (2.2) *holds. Then, the integrated volatility process,* $(IV_t)_{t\in\mathbb{N}}$*, is stationary with the following first and second-order moment structure*

$$\mathbb{E}[IV_t] = \xi,$$
$$\mathbb{E}[IV_t IV_{t+\ell}] = \xi^2 \int_0^1 (1-y)\Big(\exp\{\kappa(\ell+y)\} + \exp\{\kappa(|\ell-y|)\}\Big)dy,$$

*for* $\ell \in \mathbb{N}_0$*. In addition, suppose the following conditions hold:*

1. $\lim_{\ell\to\infty} \kappa(\ell) = 0$.
2. *There exists an integrable function* $\zeta : [-1,1] \to \mathbb{R}$ *such that* $\frac{\kappa(\ell+y)}{\kappa(\ell)} \to \zeta(y)$ *as* $\ell \to \infty$ *for any* $y \in [-1,1]$,
3. $\limsup\limits_{\ell\to\infty} \sup\limits_{y\in[-1,1]} \left|\frac{\kappa(\ell+y)}{\kappa(\ell)}\right| < \infty$.

*Then as* $\ell \to \infty$*:*

$$\mathbb{E}[(IV_t - \xi)(IV_{t+\ell} - \xi)] \sim \xi^2 \kappa(\ell) \int_{-1}^1 (1-|y|)\zeta(y)dy.$$

*Proof.* The proof can be found in [Bolko, 2021]. □

Where we denote asymptotic equivalence with $f(\ell) \sim g(\ell)$ meaning that $\frac{f(\ell)}{g(\ell)} \to 1$ as $\ell \to \infty$.

The integral describing the second-order moments of integrated volatility depends on $Y$ and might not be possible to solve analytically. Thus, one might need to approximate the integral or solve the integral numerically. Moments of higher order can also be expressed in this way, as shown in [Bolko et al., 2022], increasing the order of integration by one makes the resulting expression unwieldy to work with in practice. Therefore, estimation procedures rely on low-order moments, as showcased later.

## 2.2 Fractional Stochastic Volatility

This section is based on [Cheridito et al., 2003] and [Bolko, 2021].

In this section, a fractional Ornstein-Uhlenbeck process for $Y$ in (2.2) is introduced, in order to have a fractional stochastic volatility model, fSV. This will be the only process for $Y$ that will be considered throughout this project, and thus the volatility process will in all scenarios be driven by a fOU process.

Before introducing both the Ornstein-Uhlenbeck- and Fractional Ornstein-Uhlenbeck processes, we start by introducing the fractional Brownian motion.

A fractional Brownian motion is a zero-mean Gaussian process with continuous paths, starting from 0, with covariance structure

$$\mathbb{E}[B_s^H B_\tau^H] = \frac{1}{2}\left(|\tau|^{2H} + |s|^{2H} - |\tau - s|^{2H}\right),$$

where $H$ is the Hurst index. $H < \frac{1}{2}$ leads to negative correlation between increments, $H > \frac{1}{2}$ positive correlation and $H = \frac{1}{2}$ no correlation, i.e. a standard Brownian motion. Furthermore, the closer $H$ gets to 0, the more the paths of the fractional Brownian motion will fluctuate, why it is called rough. Oppositely, as $H$ goes toward, 1 the paths of the fractional Brownian motion will have a trendlike structure.

We are now ready to introduce the process which will be the underlying driver of the volatility process.

To motivate why the fractional version exists, the standard Ornstein-Uhlenbeck is introduced,

$$Y_\tau^{1/2} = \nu \int_{-\infty}^{\tau} e^{-\lambda(\tau - s)} dB_s, \quad \tau \geq 0, \tag{2.3}$$

where $\nu, \lambda > 0$, which is the unique solution to the Langevin equation

$$V_\tau = \xi' - \lambda \int_0^\tau V_s ds + N_\tau, \quad \tau \geq 0, \tag{2.4}$$

if the noise process is $N_\tau = \nu B_\tau$ and with initial condition $\xi' = \nu \int_{-\infty}^{0} \exp\{\lambda s\} B_s$. However, the Langevin equation can be solved pathwise for more general noise processes than the Brownian motion. For example, for each $H \in (0, 1]$ and every, $a \in [-\infty, \infty)$ there exists a pathwise Riemann-Stieltjes integral for

$$\int_a^\tau \exp\{\lambda s\} dB_s^H, \quad \tau > a,$$

which when used in the following equation

$$Y_\tau^{\xi'} = \exp\{-\lambda\tau\}\left(\xi' + \nu \int_0^\tau e^{\lambda s} dB_s^H\right), \quad \tau \geq 0, \tag{2.5}$$

is the unique almost surely continuous process that solves the equation

$$V_\tau = \xi' - \lambda \int_0^\tau V_s ds + \nu B_\tau^H, \quad \tau \geq 0. \tag{2.6}$$

In particular, in the case of positive $\tau$'s of the almost surely continuous process

$$Y_\tau = \nu \int_{-\infty}^{\tau} e^{-\lambda(\tau - s)} dB_s^H, \quad \tau \in \mathbb{R}, \tag{2.7}$$

will solve (2.6) with initial condition $\xi' = Y_0$. The stationarity of $Y_\tau$ follows from the stationarity of the increments of the fractional Brownian motion. Furthermore, for every random variable $\xi'$

$$Y_\tau - Y_\tau^{\xi'} = \exp\{-\lambda\tau\}(Y_0 - \xi') \to 0, \quad \text{as } t \to \infty \text{ a.s.},$$

which implies that every stationary solution of (2.6) has the same distribution as $(Y_\tau)_{t \geq 0}$. We call $Y_\tau^{\xi'}$ a fractional Ornstein-Uhlenbeck process with initial condition $\xi'$ and $Y_\tau$ a stationary fractional Ornstein-Uhlenbeck process [Cheridito et al., 2003].

In order to estimate the parameters in (2.7) by generalized method of moments, we need the covariance structure of the fractional stochastic volatility model as described in Section 2.1.1.

**Lemma 2**

*If $Y$ follows the model in (2.7), then for $\ell \geq 0$*

$$\kappa(0) = \frac{\nu^2}{2\lambda^{2H}}\Gamma(1+2H),$$
$$\kappa(\ell) = \kappa(0)\cosh(\lambda\ell) - \frac{\nu^2\ell^{2H}}{2}{}_1F_2(1; H+\frac{1}{2}, H+1; \frac{\lambda^2\ell^2}{4}), \quad \ell \geq 0,$$

*where ${}_qF_p(a_1,\ldots,a_p; b_1,\ldots,b_q; x)$ is the generalized hypergeometric function with $p$ parameters of type 1 and $q$ parameters of type 2.*

*Proof.* The proof can be found in [Bolko, 2021]. □

Where the generalized hypergeometric function is defined as

$${}_pF_q(a_1,\ldots,a_p; b_1,\ldots,b_q; x) = \sum_{k=0}^{\infty} \frac{(a_1)_k(a_2)_k\cdots(a_p)_k}{(b_1)_k(b_2)_k\cdots(b_q)_k}\frac{x^k}{k!},$$

and $(a)_k$ is the Pochhammer symbol

$$(a)_k \equiv \frac{\gamma(a+k)}{\gamma(a)} = a(a+1)(a+2)\cdots(a+k-1).$$

Using Theorem 1 along with Lemma 2 and a Taylor approximation, the following remark can be made.

**Remark** If $Y$ follows the model in (2.7), the second-order moment structure of integrated variance can be approximated by the following expression for $\ell \geq 1$:

$$\begin{aligned}
\mathbb{E}[IV_t^2] &\approx \xi^2\exp\{\kappa(0)\}\left(1-\kappa(0)+\frac{2\kappa(0)}{\lambda^2}(cosh(\lambda)-1) - c_1F_2(1; H+\frac{3}{2}, H+2; \frac{\lambda^2}{4})\right)\\
\mathbb{E}[IV_tIV_{t+\ell}] &\approx \xi^2\exp\{\kappa(\ell)\}\left(1-\kappa(\ell)+\frac{2\kappa(0)}{\lambda^2}cosh(\lambda\ell)(cosh(\lambda)-1)\right)\\
&\quad - \xi^2\exp\{\kappa(\ell)\}\frac{c}{2}(\ell+1)^{2H+2}{}_1F_2\left(1; H+\frac{3}{2}, H+2; \frac{\lambda^2(\ell+1)^2}{4}\right)\\
&\quad - \xi^2\exp\{\kappa(\ell)\}\frac{c}{2}(\ell-1)^{2H+2}{}_1F_2\left(1; H+\frac{3}{2}, H+2; \frac{\lambda^2(\ell-1)^2}{4}\right)\\
&\quad + \xi^2\exp\{\kappa(\ell)\}c\ell^{2H+2}{}_1F_2\left(1; H+\frac{3}{2}, H+2; \frac{\lambda^2\ell^2}{4}\right),
\end{aligned} \tag{2.8}$$

where $c = \frac{v^2}{(2H+1)(2H+2)}$.

The approximation in this remark is based on the Taylor approximation, $\exp\{\kappa(\ell+y)-\kappa(\ell))\} \approx 1+\kappa(\ell+y)-\kappa(\ell)$ for $y \in (0,1)$. The accuracy of the approximation depends on how close $\kappa(\ell+y)-\kappa(\ell))$ is to zero. The approximation is therefore fairly accurate in areas where $\kappa(\ell)$ is slowly decreasing. When $H$ is very small, the correlation function decreases fast for small $\ell$ and the accuracy of the approximation is poor. Thus, one needs to be careful with this approximation, but it is fast to calculate compared to the integral representation in Theorem 1.

With this Remark and Theorem 1 we are able to construct moment conditions.

## 2.3 Generalized Method of Moment Estimation

This section is based on [Bolko et al., 2022].

In the setup of Section 2.1, the spot volatility depends on the set of parameters, $\theta = (\xi, \phi) \in \Theta$. Denote the true parameters by $\theta_0 \in \Theta$, the probability measure induced by $\theta$ with $\mathbb{P}_\theta$ and corresponding expectation by $\mathbb{E}_\theta$. Lastly, the $\sigma$-algebra generated by $\sigma^2$ is denoted as $\mathscr{F}^\sigma$. Now to the main assumption of $Y$.

**Assumption 3**

*The process $Y$ and its covariance function $\kappa$ satisfy*

1. *$Y$ has continuous sample paths for any $\phi \in \Phi$,*
2. *$\kappa_\phi(u)$ is a continuous function.*

Condition *1.* follows naturally for Gaussian processes. Condition *2.* is important to ensure the moments are continuous with respect to $\theta$, as for these assumptions in the specific case of $Y$ following (2.7), the following remark is noted.

**Remark** For the fractional Ornstein-Uhlenbeck process described in Section 2.2 Assumption 3 condition *1.* has been shown to hold in Proposition 3.4 of [Kaarakka and Salminen, 2011]. Condition *2.* follows immediately from the continuity of the hyperbolic cosine and generalized hypergeometric function.

### 2.3.1 Consistency of Generalized Method of Moment Estimation

In this section, we introduce the required assumptions for the consistency of the GMM estimator to hold.

In order to speak on the consistency of the method of moment estimation, the structure of the moment conditions for the $IV_t$ process are

$$\begin{aligned} g_0^{(1)}(\theta) &= \mathbb{E}[IV_t(\theta)], \\ g_0^{(2)}(\theta) &= \mathbb{E}[IV_t^2(\theta)], \\ g_\ell(\theta) &= \mathbb{E}[IV_t(\theta)IV_{t-\ell}(\theta)], \quad \ell \in \mathbb{Z}, \quad \theta \in \Theta. \end{aligned}$$

Fix some $k \in \mathbb{N}$, then we can denote the $k+2$ long vector of moments as

$$G(\theta) = \Big(g_0^{(1)}(\theta), g_0^{(2)}(\theta), g_1(\theta), \dots, g_k(\theta)\Big)^\top, \quad \theta \in \Theta.$$

We will focus on the double asymptotic case, i.e. when $n \to \infty$ and $T \to \infty$. Where $T$ is the number of days and $n$ is the number of observations for each day. Under the double asymptotic setup, we can use a consistent estimator of the integrated volatility $IV_t$, and denote this estimator by $V_t^n$. Then, for some fixed $k \in \mathbb{N}$, denote

$$\begin{aligned} \mathbb{IV}_t &= \left(IV_t, IV_t^2, IV_t IV_{t-1}, \dots, IV_t IV_{t-k}\right)^\top \\ \mathbb{V}_t^n &= \left(V_t^n, (V_t^n)^2, V_t^n V_{t-1}^n, \dots, V_t^n V_{t-k}^n\right)^\top, \end{aligned}$$

and define the random function associated with the sample moments

$$\widetilde{m}_{n,T}(\theta) = \frac{1}{T}\sum_{t=1}^{\top} \mathbb{V}_t^n - G(\theta),$$

and resulting in the GMM estimator

$$\widetilde{\theta}_{n,T} = \arg\min_{\theta\in\Theta} \widetilde{m}_{n,T}(\theta)^\top \mathbb{W}_{n,T}\widetilde{m}_{n,T}(\theta).$$

We introduce a standard assumption about the limiting behavior of $\mathbb{W}_T$.

**Assumption 4**

*$\mathbb{W}_T = A_T^\top A_T$ for a random $(k+2)\times(k+2)$ matrix $A_T$, which under $\mathbb{P}_{\theta_0}$ converges almost surely to a non-random matrix $A$ as $T \to \infty$.*

We also introduce an assumption about the parameters being identifiable.

**Assumption 5**

*$A\mathbb{E}_{\theta_0}[\widetilde{m}_{n,T}(\theta)] = 0$ if and only if $\theta = \theta_0$.*

Assumption 5 is a standard identification condition in GMM that ensures uniqueness of the solution. It is hard to check when moments are not given in algebraic form.

**Assumption 6**

*The processes $(IV_t)_{t\in\mathbb{Z}}$ and $(V_t^n)_{t\in\mathbb{Z},n\in\mathbb{N}}$ admit the following:*

1. *$(IV_t)_{t\in\mathbb{Z}}$ is a stationary and ergodic process under $\mathbb{P}_\theta$ for any $\theta \in \Theta$,*
2. *$\sup_{t\in\mathbb{Z}} \mathbb{E}_{\theta_0}[(V_t^n - IV_t)^2] \to 0$ as $n \to \infty$.*

Now we are ready to present the consistency of $\widetilde{\theta}_{n,T}$.

**Theorem 7**

*Suppose Assumption 3, 4, 5 and 6 hold. As $T \to \infty$ and $n \to \infty$*

$$\widetilde{\theta}_{n,T} \xrightarrow{\mathbb{P}} \theta_0.$$

Thus, under the assumptions, the estimator is consistent.

If one were to use realized volatility as an estimator for integrated volatility then under a boundedness condition on drift and volatility, Assumption 6 condition *2.* holds, since

$$\sup_{t\in\mathbb{Z}} |\mathbb{E}[(RV_t^n - IV_t)^2]| \le Cn^{-1}, \tag{2.9}$$

for some $C > 0$.

### 2.3.2 Asymptotic Normality of GMM Estimator

This Section is based on [Bolko et al., 2022].

With the consistency of the generalized method of moment estimation setup shown in Section 2.3.1, we will now look at the asymptotic normality of the method.

Initially we need to assume that under $\mathbb{P}_{\theta_0}$, the process $Y$ has a causal moving average representation of the form

$$Y_t = \int_{-\infty}^{t} K(t-u)dB_u, \quad t \in \mathbb{R}, \tag{2.10}$$

where $B = (B_t)_{t\in\mathbb{R}}$ is a two-sided Brownian motion, defined as

$$B_t = \begin{cases} B_t^1, & t > 0, \\ 0, & t = 0, \\ B_{-t}^2, & t < 0, \end{cases}$$

with $B^1$ and $B^2$ being two independent Brownian motions. As well as some measurable kernel $K : (0,\infty) \to \mathbb{R}$, such that $\int_0^\infty K(u)^2 du < \infty$, with an extension to the entire real line by setting $K(u) = 0$ for $u < 0$.

The fractional Ornstein-Uhlenbeck process introduced in Section 2.2 has the causal moving average representation from (2.10), this is shown in [Barndorff-Nielsen and Basse-O'Connor, 2011].

The asymptotic behavior of $K(u)$ as $u \to \infty$ dictates the long-term memory of $Y$. To derieve the asymptotic normality of our GMM estimator, we need to constrain that memory.

**Assumption 8**

*$K(u) = O(u^{-\gamma})$ as $u \to \infty$ for some $\gamma > 1$.*

[Garnier and Sølna, 2018] showed that the kernel in (2.10) as $u \to \infty$, is proportional to $u^{H-3/2}$ for $H \in (0, \frac{1}{2})$. Moreover, the fOU process from (2.7) with $H = \frac{1}{2}$ implies $K(u) = \nu \exp\{-\lambda u\} = o(u^{-\gamma})$, for all $\gamma > 1$ as $u \to \infty$. Thereby the fSV model requires $H \leq \frac{1}{2}$ to be covered by Assumption 8 allowing for rough volatility but ruling out the long-memory version.

Furthermore, if $K(u)$ is asymptotically proportional to $u^{-\gamma}$ for $y \in (0,1)$ e.g. with the fSV model for $H > 1/2$, then asymptotic normality with a standard rate of convergence ceases to hold.

Further assumptions are needed for the asymptotic distribution of $\widetilde{\theta}_{n,T}$.

Define $g : \mathbb{R}^{k+2} \times \Theta \to \mathbb{R}$ as

$$g(x, \theta) = x - G(\theta).$$

**Assumption 9**

1. *$\theta_0$ is an interior point of $\Theta$.*
2. *$J^\top \mathbb{W} J$ is invertible, where $J = \mathbb{E}_{\theta_0}[\nabla_\theta g(\mathbb{V}_1^n, \theta_0)]$ and $\mathbb{W} = A^\top A$.*
3. *The function $\theta \mapsto g(x, \theta)$ is continuously differentiable as well as $\mathbb{E}_{\theta_0}[\|g(\mathbb{V}_1^n, \theta_0)\|^2] < \infty$ and $\mathbb{E}_{\theta_0}[\sup_{\theta\in\Theta} \|\nabla_\theta g(\mathbb{V}_1^n, \theta)\|] < \infty$.*

We also need assumptions on the integrated volatility process $(IV_t)_{t\in\mathbb{Z}}$ and corresponding estimator $(V_t^n)_{t\in\mathbb{Z},n\in\mathbb{N}}$.

**Assumption 10**

*$\sup_{t\in\mathbb{Z}} \mathbb{E}_{\theta_0}[(\sqrt{T}(V_t^n - IV_t))^2] \to 0$ as $T \to \infty$ and $n \to \infty$.*

We now have the necessary assumptions to be able to present the asymptotic distribution of $\widetilde{\theta}_{n,T}$.

**Theorem 11**

*Suppose Assumptions 3, 4, 5, 6, 8, 9 and 10. As $T \to \infty$ and $n \to \infty$,*

$$\sqrt{T}(\widetilde{\theta}_{n,T} - \theta_0) \xrightarrow{d} N(0, (J^\top \mathbb{W} J)^{-1} J^\top \mathbb{W} \Sigma_{\mathbb{IV}} \mathbb{W} J (J^\top \mathbb{W} J)^{-1}), \tag{2.11}$$

*where*

$$\Sigma_{\mathbb{IV}} = \sum_{\ell=-\infty}^{\infty} \Gamma_{\mathbb{IV}}(\ell),$$

*and*

$$\Gamma_{\mathbb{IV}}(\ell) = \mathbb{E}_{\theta_0}[(\mathbb{IV}_1 - G(\theta_0))(\mathbb{IV}_{1+\ell} - G(\theta_0))^\top]$$

*Proof.* The proof can be found in [Bolko et al., 2022]. □

In traditional GMM estimation fashion, we seek to minimize the asymptotic variance in (2.11) to achieve an efficient estimator. In order to do this, we need a consistent estimator of $\Sigma_{\mathbb{IV}}$, such that the weight matrix $\mathbb{W}$ can be chosen as the inverse. To this end, a HAC-type estimator will be used

$$\widehat{\Sigma}_{\mathbb{IV}} = \widehat{\Gamma}(0) + \sum_{\ell=1}^{T-1} w(\ell/L)[\widehat{\Gamma}(\ell) + \widehat{\Gamma}(\ell)^\top], \tag{2.12}$$

with

$$\widehat{\Gamma}(\ell) = \frac{1}{T}\sum_{t=1}^{T-\ell}(\mathbb{V}_t^n - G(\widetilde{\theta}_{n,T}))^\top(\mathbb{V}_{t+\ell}^n - G(\widetilde{\theta}_{n,T})). \tag{2.13}$$

Where $w$ is a weight function and $L = o(T^{1/2})$ is the lag length.

Some assumptions are needed for the weight function $w$

**Assumption 12**

1. *$w(0) = 1$ and $\sup_{x\geq 0} |w(x)| < \infty$.*
2. *$w$ is continuous at $0$.*
3. *$\int_0^\infty \overline{w}(x)dx < \infty$ where $\overline{w}(x) = \sup_{y\geq x} |w(y)|$.*

Assumption 12 is fulfilled by the Bartlett kernel, which is also the choice of kernel in our application of the GMM setup.

We can now choose the weight matrix $\mathbb{W} = \widehat{\Sigma}_{\mathbb{IV}}^{-1}$ and thereby minimize the variance of (2.11), thus achieving an efficient estimator.

**Theorem 13**

*Under the same assumptions as in Theorem 11 and with a consistent estimator for $\Sigma_{\mathbb{IV}}$, then as $T \to \infty$ and $n \to \infty$*

$$\sqrt{T}(\widetilde{\theta}_{n,T} - \theta_0) \xrightarrow{d} N(0, (J^\top \Sigma_{\mathbb{IV}}^{-1} J)^{-1}).$$

*Proof.* The proof can be found in [Bolko et al., 2022]. □

With the results shown in this section, we now have the distribution of the GMM estimator.

## 2.4 Microstructure Noise

In practice, Microstructure noise leads to a departure from the semimartingale model in (2.1). Microstructure noise is primarily caused by the bid-ask spread bounce. Hence, what is observed is a noisy version of $X$ from (2.1), which we define as

$$Z_\tau = X_\tau + \varepsilon_\tau \tag{2.14}$$

where $\varepsilon_\tau$ is assumed to be an i.i.d. process and $X \perp\!\!\!\perp \varepsilon$.

The process $\varepsilon$ is assumed to satisfy

$$\mathbb{E}(\varepsilon_\tau) = 0,$$
$$\mathbb{E}(\varepsilon_\tau^2) = \psi.$$

### 2.4.1 Microstructure Noise Robust Estimator for $IV$

If one were to use realized volatility as an estimator for integrated volatility, the expression would be dominated by the variance for the microstructure noise as $n \to \infty$. Let $\Delta_i^n X = X_{\frac{i}{n}} - X_{\frac{i-1}{n}}$ then

$$\begin{aligned}\frac{1}{2n}\sum_{i=1}^n \Delta_i^n (X+\varepsilon)^2 &= \frac{1}{2n}\sum_{i=1}^n (\Delta_i^n X)^2 + \frac{1}{2n}\sum_{i=1}^n (\Delta_i^n \varepsilon)^2 + \frac{1}{n}\sum_{i=1}^n \Delta_i^n X \Delta_i^n \varepsilon \\ &\xrightarrow{p} \psi,\end{aligned} \tag{2.15}$$

thus, in the presence of microstructure noise, we need a different estimator for $IV_t$, the estimator of choice will be Modulated Realized Covariance, MRC, which builds on the idea of averaging the data over some period within a given range, thereby reducing the impact of the microstructure noise. Then using a scaled realized volatility estimator on the pre-averaged data, and lastly do a bias correction. The MRC estimator has a convergence rate of $n^{1/4}$. Related to this MRC estimator is whether a bias correction is included, a parameter $\theta$ and a parameter $\delta$. In this project, MRC with a bias correction, $\delta = 0$ and $\theta = 0.3$ is used, the parameter choice for MRC is based on the simulation study performed in [Andreassen and Dam, 2021]. For more detail about this estimator, see [Christensen et al., 2010].

### 2.4.2 Microstructure Noises Effect on GMM

Previous papers on GMM estimation of Rough volatility models are few, and far between. To our knowledge, do there not exist any papers that have used GMM estimation of rough volatility models in presence of microstructure noise. In [Bolko et al., 2022], they estimated roughness with GMM estimation, however microstructure noise was not added during their simulation study. This is what this paper intent to. We are going to check the distribution for $\widehat{\theta}_{n,T}$ in the presence of microstructure noise with different choices of estimators for $IV_t$ and see if Theorem 13 still seems valid and thereby validate the GMM approach for different estimators of $IV_t$.

Chapter 3

# Simulation Study

This section is based on [Bolko et al., 2022].

In this chapter, we will do a simulation study as to gauge the finite sample properties of the GMM approach of estimating parameters for the model setup from (2.1) and (2.2) with the fractional Ornstein-Uhlenbeck process described in Section 2.2 as the $Y$ in the presence of microstructure noise and without. Thus, we can assess the accuracy of the estimation and validate the GMM approach in the presence of microstructure noise.

### Model specification

We assume the log-price without microstructure noise, $X_\tau$, evolves as a driftless Itô process

$$dX_\tau = \sigma_\tau dW_\tau, \quad \tau \geq 0, \tag{3.1}$$

with initial condition $X_0 = 0$. The term $\sigma_\tau$ is the spot volatility and $W_\tau$ is a standard Brownian motion. We discretize X via an Euler Scheme. The log-variance, $Y_\tau = \log\left(\sigma_\tau^2\right)$ is a fOU process given as

$$dY_\tau = -\lambda(Y_\tau - \eta)d\tau + \nu dB_\tau^H, \tag{3.2}$$

where $B_\tau^H$ is a fractional Brownian Motion and $W \perp\!\!\!\perp B^H$. Where the initial value of $Y$ is random and distributed as $Y_0 \sim N(\eta, \kappa(0))$.

The SDE in (3.2) is solved to get a more convenient expression for $Y$

$$Y_\tau = \eta + (Y_{\tau-\Delta} - \eta)\exp\{\lambda\Delta\} + \nu \int_{\tau-\Delta}^{\tau} \exp\{-\lambda(\tau - s)\} dB_s^H. \tag{3.3}$$

This is not entirely trivial, since we are dealing with a fractional Brownian motion, however in [Cheridito et al., 2003] it is shown that it works.

The stochastic integral is approximated as $\int_{\tau-\Delta}^{\tau} \exp\{-\lambda(\tau - s)\} dB_s^H \approx \exp\{-\lambda\Delta/2\}(B_\tau^H - B_{\tau-\Delta}^H)$ meaning that increments to a discretely sampled fractional Brownian motion are required. In this simulation study, we have used circulant embedding to get an exact discretization of paths from a fractional Brownian motion, see [Asmussen and Glynn, 2007], this method is among the fastest methods for exact discretization of fractional Brownian motions, with a complexity of $O(T \cdot n \ \log(T \cdot n))$.

The log-price in the presence of microstructure noise is given as

$$Z_\tau = X_\tau + \varepsilon_\tau. \tag{3.4}$$

**Parameter specification**

We have chosen to make two scenarios, for both scenarios we make 1000 replications with 23400 equidistant observations per day, in the first scenario we have 100 days, in the second we have 1000. The initial value of $Y$ is drawn from its stationary distribution $Y_0 \sim N(\eta, \kappa(0))$. Where $\eta = \mathbb{E}[Y_0]$ is

$$\begin{aligned} \mathbb{E}[\exp\{Y_0\}] &= \xi \\ \exp\left\{\eta + \frac{1}{2}\kappa(0)\right\} &= \xi \Rightarrow \\ \eta &= \log(\xi) - \frac{1}{2}\kappa(0). \end{aligned}$$

Recall that $\mathbb{E}[\sigma_t^2] = \xi$, and we set $\xi = 0.025$. For the Hurst index, we have chosen $H = [0.05, 0.2, 0.3, 0.4]$. For the lag-parameter, we have chosen $\ell = (1, 2, 3, 4, 5, 10, 15)$. For the variance of the microstructure noise, we have decided to make it constant for within a day, but different from day to day. Furthermore there is a relationship between the variance of returns and the variance of microstructure noise, which is described in [Bandi and Russell, 2006]. We set the variance of the microstructure noise to

$$\omega_t = 0.01 \cdot \sqrt{\frac{1}{n}\sum_{s=1}^{n=23400} \sigma_s^4} \tag{3.5}$$

$$\varepsilon_\tau \sim N(0, \omega_t), \quad \tau \in [t-1, t] \tag{3.6}$$

The subscript $s$ refers to all observations between $t-1$ and $t$.

**Initial Guesses and Optimization Procedure**

For the optimization procedure, we want the initial guesses to be qualified, both since it will possibly cost fewer iterations to complete the procedure, and it increases the chances of reaching the global minimum. We denote the initial values by $\theta_{ini} = (\xi_{ini}, \lambda_{ini}, \nu_{ini}, H_{ini})$. The value for $\xi_{ini}$ is chosen to be the average of the estimated integrated volatility. Initializing $H$ and $\nu$ is a bit more complicated. We exploit the auxiliary two-stage procedure proposed in [Gatheral et al., 2018], which relies on the scaling law

$$\frac{\gamma_h}{|h|^{qH}} = \frac{\mathbb{E}[|Y_{t+h} - Y_t|^q]}{|h|^{qH}} \to K_q \nu^q \tag{3.7}$$

as $h \to 0$, where $K_q = 2^{q/2}\frac{\Gamma(\frac{q+1}{2})}{\sqrt{\pi}}$ is the $q$'th moment of the absolute value of a standard normal random variable. This entails a log-linear relationship between $\gamma_h$ and $|h|$ i.e. $\log(\gamma_h) = \log(K_q\nu^q) + qH\log(|h|)$. We employ $V_t^n$ as a proxy for the instantaneous variance and substitute the left-hand side of (3.7) by the sample mean

$$\widehat{\gamma}_h = \frac{1}{T-m}|\log(V_{t+h}^n) - \log(V_t^n)|^q. \tag{3.8}$$

For $h = 1, \dots, m$, $q = 2$ and $m = 6$.

We can now regress $\log(\widehat{\gamma})$ on $\log(|h|)$ while allowing for an intercept to achieve $\widehat{\beta}_0$ and $\widehat{\beta}_1$, then isolate $\nu$ and $H$.

$$\nu_{ini} = \left( \frac{\exp\left\{ \widehat{\beta}_0 \right\}}{K_q} \right)^{\frac{1}{q}}, \qquad H_{ini} = \frac{\widehat{\beta}_1}{q}.$$

The parameter $\lambda$ is pre-estimated such that the theoretical variance of $Y_t$ equals the sample variance of $\log(V_t^n)$, thus we construct the function

$$f(\lambda) = |(\frac{\nu^2}{2\lambda^{2H}}\Gamma(1+2H) - var(\log(V_t^n))|,$$

where $H$ and $\nu$ are the initial guesses obtained by the regression. We find the $\lambda$ which minimizes the function, and set this to $\lambda_{ini}$.

Lastly, we need to solve

$$\widetilde{\theta}_{n,T} = \arg\min_{\theta\in\Theta} \widetilde{m}_{n,T}(\theta)^\top \mathbb{W}_{n,T}\widetilde{m}_{n,T}(\theta),$$

which can be formulated as an optimization problem. The optimization algorithm used is Nelder-Mead for the first scenario and BFGS for the second. When approximating the theoretical moments $G(\theta)$, we use the approximations from (2.8).

**Estimators for $IV_t$**

The estimators we are using for $IV_t$ are realized volatility, RV, realized volatility with 5 minute sampling, RV5, and modulated realized covariance with a bias correction and $\theta = 0.3$, MRC.

**Methods of Validating the Distribution**

In this section, we will lay out the groundwork needed to investigate the distribution of the estimated parameters in a finite sample setup, as to compare with the asymptotic result from Theorem 13.

The validation is done by two slightly different methods.

For the first method, we start by Cholesky decomposing the matrix $(J^\top \Sigma_{\mathbb{IV}}^{-1} J)^{-1}$. For ease of notation, we denote $(J^\top \Sigma_{\mathbb{IV}}^{-1} J)^{-1} = \Omega = L^\top L$ where $L^\top L$ is the Cholesky decomposition, and let $L^{\top^{-1}} = L^{-\top}$.

By Theorem 13 as $T \to \infty$ and $n \to \infty$

$$L^{-\top}(\sqrt{T}(\widetilde{\theta}_{n,T} - \theta_0)) \xrightarrow{d} N(0, I).$$

Thus $L^{-\top}(\sqrt{T}(\widetilde{\theta}_{n,T} - \theta_0))$ is normally distributed where each entry is a univariate standard normal distribution.

However, we do not know either $J^\top$ and $\Sigma_{\mathbb{IV}}^{-1}$ which complicates the Cholesky decomposition. Therefore, we use the previously mentioned HAC-type estimator for $\Sigma_{\mathbb{IV}}$ from (2.12) and (2.13).

The matrix $J$ is estimated by finite central differencing evaluated at $\widetilde{\theta}_{n,T}$, we denote the estimated $J$ by $\widehat{J}$.

We do this for each repetition, let $\widehat{J}_i$, $\widehat{\Sigma}_{\mathbb{IV},i}$, $L_i$ and $\widetilde{\theta}_{n,T,i}$ refer to the matrices and parameters estimated at repetition number $i$ respectively.

We thereby achieve $L_i$ by the Cholesky decomposition $L_i^\top L_i = (J_i^\top \Sigma_{\mathbb{IV},i}^{-1} J_i)^{-1}$ and compute the test statistic for repetition $i$ as $L_i^{-\top}(\sqrt{T}(\widetilde{\theta}_{n,T,i} - \theta_0))$, we can then investigate the distribution of each of the parameters. This method however, is numerically sensitive due to the inversion of $\Sigma_{\mathbb{IV},i}$ and $(J_i^\top \Sigma_{\mathbb{IV},i} J_i)$, the Cholesky decomposition and lastly the inversion of $L_i^\top$. This approach requires that the estimate $\Omega_i$ is positive definite due to the inversion of $L_i^\top$.

The second approach relies on the fact that

$$\left(RJ\sqrt{T}(\widetilde{\theta}_{n,T} - \theta_0))\right)^\top RJ(\sqrt{T}(\widetilde{\theta}_{n,T} - \theta_0)) \xrightarrow{d} \chi^2(4)$$
$$\left\| RJ(\sqrt{T}(\widetilde{\theta}_{n,T} - \theta_0)) \right\|^2 \xrightarrow{d} \chi^2(4).$$

Thus, we get the test statistics $\left\| R_i J_i(\sqrt{T}(\widetilde{\theta}_{n,T,i} - \theta_0)) \right\|^2$ for each repetition. This procedure will be better in the sense of numerical robustness compared to the first, since only one inversion is needed. However, one loses the ability to investigate each parameter individually. Furthermore, since $\Sigma_{\mathbb{IV}}$ is a covariance matrix, therefore, by definition, positive semi definite, which implies that the $\Sigma_{\mathbb{IV}}^{-1}$ is positive semi definite as well, thus the Cholesky decomposition $\Sigma_{\mathbb{IV}}^{-1} = R^\top R$ exists. Which makes the second approach require one less assumption.

**Summary**

To get a brief overview of the model- and parameter specification, the initial guesses, the optimization procedure, the estimators for $IV_t$, and the test statistics, we present this summary.

- Log-Price without microstructure noise: $dX_\tau = \sigma_\tau dW_\tau, \quad \tau \geq 0$.
- Log-variance: $dY_\tau = -\lambda(Y_\tau - \eta)d\tau + \nu dB_\tau^H$.
- Log-price with microstructure noise: $Z_\tau = X_\tau + \varepsilon_\tau$.
- $n = 23400$.
- $T = 100$ or $T = 1000$.
- $Y_0$ drawn from $N(\eta, \kappa(0))$, where $\eta = \log(\xi) - \frac{1}{2}\kappa(0)$.
- $\xi = 0.025$.
- $\varepsilon_\tau \sim N(0, \omega_t)$, where $\omega_t = 0.01 \cdot \sqrt{\frac{1}{n}\sum_{s=1}^{n=23400} \sigma_s^4}$ .
- $H = [0.05, 0.2, 0.3, 0.4]$.
- $\ell = (1, 2, 3, 4, 5, 10, 15)$.
- $\xi_{ini} = \frac{1}{T}\sum_{t=1}^{T} V_t^n$.
- $\nu_{ini} = (\frac{\exp\{\widehat{\beta}_0\}}{K_q})^{\frac{1}{q}}$.
- $H_{ini} = \frac{\widehat{\beta}_1}{q}$.
- $\lambda_{ini} = \underset{\lambda}{\text{argmin}}|(\frac{\nu_{ini}^2}{2\lambda^{2H_{ini}}}\Gamma(1 + 2H_{ini}) - var(\log(V_t^n))|$.
- $\widetilde{\theta}_{n,T} = \arg\min_{\theta\in\Theta} \widetilde{m}_{n,T}(\theta)^\top \mathbb{W}_{n,T}\widetilde{m}_{n,T}(\theta)$ (Nelder-Mead or BFGS).
- $IV_t$ estimators:
  - RV: realized volatility
  - RV5: realized volatility with 5 min sampling.
  - MRC: Modulated realized covariance with bias correction and $\theta = 0.3$.
- Test statistics:
  - $L_i^{-\top}(\sqrt{T}(\widetilde{\theta}_{n,T,i} - \theta_0))$
  - $\left\| R_i J_i(\sqrt{T}(\widetilde{\theta}_{n,T,i} - \theta_0)) \right\|^2$

## 3.1 Simulation Results

### 3.1.1 Short Timeframe

In this section, we present tables containing the results from the setup described in Chapter 3.

Using the setup of $T = 100$, $n = 23400$ and 1000 replications, we have investigated 4 different sets of parameters.

1. Panel A: $\xi = 0.0225$, $\lambda = 0.005$, $\nu = 1.25$ and $H = 0.05$, with results found in Table 3.1.
2. Panel B: $\xi = 0.0225$, $\lambda = 0.015$, $\nu = 0.5$ and $H = 0.2$, with results found in Table 3.2.
3. Panel C: $\xi = 0.0225$, $\lambda = 0.015$, $\nu = 0.5$ and $H = 0.3$, with results found in Table 3.3.
4. Panel D: $\xi = 0.0225$, $\lambda = 0.035$, $\nu = 0.3$ and $H = 0.4$, with results found in Table 3.4.

In Section 3.1.2 we investigate the effects of increasing $T$ to 1000, which should result in a better GMM estimation, the results of this setup are summarized in Tables 3.5, 3.6, 3.7 and 3.8.

When microstructure noise is not present. Both using RV, RV5 and MRC provide somewhat decent estimates, it is hard to single one estimator as being better than the others. Estimation of $\lambda$ seems to be the weakest point, especially in Table 3.1, where the all the $\lambda$ estimates are at least twice the true value. Estimation of $H$ is also inaccurate in Tables 3.1 and 3.4. Interestingly enough, the estimates of $H$ are fairly similar in all the tables, even though the true values changes.

The story is a bit different when microstructure noise is present. When RV is the estimator for $IV_t$, the $\xi$ estimates are far higher than the true value, this is what one would expect and this is due to realized volatility being dominated by the variance of the microstructure noise if sampling is frequent enough, this phenomenon is also seen in (2.15). The same dynamic can be seen when RV5 is used as an estimator for $IV_t$, however this is to a far lesser extent. Microstructure noise does not really seem to affect estimation of $\lambda$, $nu$ nor $H$. In addition, the standard deviations are, for all parameters, generally higher in the presence of microstructure noise.

When microstructure noise is present, choosing MRC as the estimator for $IV_t$ seems to be the superior choice.

Keep in mind, that $T = 100$, thus, this might hardly be considered as asymptotic and the variance of the estimates is rather high, which follows from Theorem 13.

| Parameter | | $\xi$ | $\lambda$ | $\nu$ | $H$ |
|---|---|---|---|---|---|
| True | | 0.0225 | 0.005 | 1.25 | 0.05 |
| IV | Initial | 0.113 (0.503) | 0.0594 (0.0323) | 0.471 (0.0849) | 0.257 (0.0734) |
| | Estimate | 0.104 (0.467) | 0.013 (0.0599) | 0.559 (0.135) | 0.115 (0.0674) |
| No microstructure noise | | | | | |
| RV | Initial | 0.113 (0.503) | 0.0594 (0.0323) | 0.471 (0.0848) | 0.256 (0.0734) |
| | Estimate | 0.101 (0.429) | 0.0131 (0.0581) | 0.563 (0.132) | 0.119 (0.156) |
| RV5 | Initial | 0.114 (0.503) | 0.0522 (0.0335) | 0.533 (0.0831) | 0.213 (0.0751) |
| | Estimate | 0.1 (0.427) | 0.0114 (0.0316) | 0.562 (0.132) | 0.118 (0.0679) |
| MRC | Initial | 0.112 (0.493) | 0.0575 (0.0327) | 0.487 (0.0845) | 0.245 (0.0744) |
| | Estimate | 0.0998 (0.425) | 0.0123 (0.0424) | 0.56 (0.129) | 0.121 (0.111) |
| With microstructure noise | | | | | |
| RV | Initial | 74.4 (329) | 0.0585 (0.0326) | 0.482 (0.0885) | 0.249 (0.0721) |
| | Estimate | 61.6 (298) | 0.0227 (0.124) | 0.553 (0.276) | 0.161 (0.312) |
| RV5 | Initial | 0.359 (1.58) | 0.0524 (0.0332) | 0.541 (0.0835) | 0.21 (0.0742) |
| | Estimate | 0.318 (1.45) | 0.0121 (0.041) | 0.562 (0.144) | 0.116 (0.0963) |
| MRC | Initial | 0.112 (0.493) | 0.0571 (0.0328) | 0.49 (0.0844) | 0.243 (0.0746) |
| | Estimate | 0.102 (0.456) | 0.0125 (0.0411) | 0.561 (0.133) | 0.117 (0.0674) |

***Table 3.1.*** Panel A. Scenario one

| Parameter | | $\xi$ | $\lambda$ | $\nu$ | $H$ |
|---|---|---|---|---|---|
| True | | 0.0225 | 0.015 | 0.5 | 0.2 |
| IV | Initial | 0.032 (0.0348) | 0.0621 (0.0316) | 0.329 (0.0815) | 0.358 (0.0717) |
| | Estimate | 0.0303 (0.034) | 0.00846 (0.0247) | 0.549 (0.17) | 0.114 (0.0882) |
| No microstructure noise | | | | | |
| RV | Initial | 0.032 (0.0348) | 0.062 (0.0316) | 0.33 (0.0814) | 0.358 (0.0716) |
| | Estimate | 0.0301 (0.0335) | 0.0085 (0.0251) | 0.554 (0.161) | 0.112 (0.077) |
| RV5 | Initial | 0.032 (0.0349) | 0.051 (0.0332) | 0.401 (0.0786) | 0.276 (0.0743) |
| | Estimate | 0.03 (0.0348) | 0.00977 (0.0345) | 0.542 (0.135) | 0.116 (0.0709) |
| MRC | Initial | 0.0317 (0.0345) | 0.059 (0.0323) | 0.347 (0.0812) | 0.335 (0.0718) |
| | Estimate | 0.0302 (0.0367) | 0.00815 (0.0216) | 0.55 (0.148) | 0.113 (0.0693) |
| With microstructure noise | | | | | |
| RV | Initial | 15.6 (16.9) | 0.0617 (0.0317) | 0.332 (0.0841) | 0.356 (0.0711) |
| | Estimate | 12.5 (14.1) | 0.0193 (0.115) | 0.428 (0.307) | 0.171 (0.233) |
| RV5 | Initial | 0.0839 (0.0918) | 0.0499 (0.0333) | 0.411 (0.0779) | 0.267 (0.072) |
| | Estimate | 0.0777 (0.0908) | 0.00894 (0.0233) | 0.541 (0.128) | 0.117 (0.0581) |
| MRC | Initial | 0.0317 (0.0344) | 0.0584 (0.0324) | 0.35 (0.0808) | 0.33 (0.0716) |
| | Estimate | 0.0302 (0.0364) | 0.00811 (0.0214) | 0.548 (0.15) | 0.112 (0.0664) |

***Table 3.2.*** Panel B. Scenario one

| Parameter | | $\xi$ | $\lambda$ | $\nu$ | $H$ |
|---|---|---|---|---|---|
| True | | 0.0225 | 0.015 | 0.5 | 0.3 |
| IV | Initial | 0.0592 (0.2) | 0.0615 (0.0313) | 0.396 (0.161) | 0.426 (0.071) |
| | Estimate | 0.0561 (0.29) | 0.023 (0.0897) | 0.64 (0.236) | 0.155 (0.131) |
| No microstructure noise | | | | | |
| RV | Initial | 0.0591 (0.2) | 0.0615 (0.0313) | 0.396 (0.161) | 0.425 (0.0711) |
| | Estimate | 0.0611 (0.327) | 0.0213 (0.0695) | 0.643 (0.237) | 0.15 (0.129) |
| RV5 | Initial | 0.059 (0.198) | 0.0521 (0.0331) | 0.46 (0.153) | 0.352 (0.0749) |
| | Estimate | 0.0539 (0.25) | 0.022 (0.0932) | 0.64 (0.217) | 0.152 (0.108) |
| MRC | Initial | 0.0586 (0.198) | 0.0591 (0.0319) | 0.411 (0.159) | 0.406 (0.072) |
| | Estimate | 0.051 (0.165) | 0.024 (0.121) | 0.643 (0.215) | 0.153 (0.13) |
| With microstructure noise | | | | | |
| RV | Initial | 28.6 (96.8) | 0.0612 (0.0314) | 0.399 (0.168) | 0.422 (0.0704) |
| | Estimate | 21.4 (81.5) | 0.0663 (0.473) | 0.546 (0.369) | 0.214 (0.938) |
| RV5 | Initial | 0.154 (0.523) | 0.0512 (0.0331) | 0.468 (0.156) | 0.344 (0.0739) |
| | Estimate | 0.133 (0.502) | 0.0232 (0.0906) | 0.643 (0.215) | 0.152 (0.152) |
| MRC | Initial | 0.0586 (0.198) | 0.0586 (0.032) | 0.414 (0.159) | 0.402 (0.0719) |
| | Estimate | 0.0548 (0.206) | 0.0241 (0.14) | 0.644 (0.214) | 0.154 (0.177) |

***Table 3.3.*** Panel C. Scenario one

| Parameter | | $\xi$ | $\lambda$ | $\nu$ | $H$ |
|---|---|---|---|---|---|
| True | | 0.0225 | 0.035 | 0.3 | 0.4 |
| IV | Initial | 0.0305 (0.0347) | 0.0601 (0.0282) | 0.273 (0.162) | 0.49 (0.0649) |
| | Estimate | 0.028 (0.0382) | 0.0242 (0.108) | 0.474 (0.303) | 0.215 (0.284) |
| No microstructure noise | | | | | |
| RV | Initial | 0.0305 (0.0347) | 0.06 (0.0283) | 0.273 (0.162) | 0.489 (0.065) |
| | Estimate | 0.0281 (0.0384) | 0.0272 (0.15) | 0.481 (0.3) | 0.209 (0.358) |
| RV5 | Initial | 0.0305 (0.0347) | 0.0417 (0.0298) | 0.357 (0.152) | 0.35 (0.0746) |
| | Estimate | 0.0299 (0.0636) | 0.0193 (0.0671) | 0.561 (0.225) | 0.151 (0.114) |
| MRC | Initial | 0.0302 (0.0344) | 0.0545 (0.0292) | 0.294 (0.159) | 0.448 (0.0678) |
| | Estimate | 0.0282 (0.0399) | 0.0252 (0.111) | 0.516 (0.293) | 0.18 (0.208) |
| With microstructure noise | | | | | |
| RV | Initial | 14.5 (16.5) | 0.0598 (0.0283) | 0.276 (0.17) | 0.487 (0.0649) |
| | Estimate | 10.2 (14.3) | 0.0407 (0.187) | 0.359 (0.342) | 0.243 (0.272) |
| RV5 | Initial | 0.0788 (0.0909) | 0.0401 (0.0301) | 0.37 (0.154) | 0.336 (0.0748) |
| | Estimate | 0.0768 (0.127) | 0.0256 (0.108) | 0.576 (0.223) | 0.143 (0.0979) |
| MRC | Initial | 0.0302 (0.0345) | 0.0535 (0.0293) | 0.298 (0.159) | 0.44 (0.0683) |
| | Estimate | 0.0284 (0.041) | 0.0243 (0.108) | 0.521 (0.29) | 0.163 (0.138) |

***Table 3.4.*** Panel D. Scenario one

**Distribution of Estimates**

The color schemes in the following figures will refer to different sets of true values, as well as either a standard normal or $\chi^2(4)$ distribution for reference. The color scheme is as follows

- Red: Panel A.
- Green: Panel B.
- Blue: Panel C.
- Purple: Panel D.
- Black: Standard normal distribution or $\chi^2(4)$ distribution.

In Figure 3.1, 3.2 and 3.3 we show the distribution of each parameter obtained by the first method. In Figure 3.4 the distribution of the test statistic for the second method is plotted. For both methods, we only keep the 90 percent absolute smallest test statistics.

In Figure 3.1 we see the distribution of $\xi, \lambda, \nu$ and $H$ in that order, this is done with MRC as estimator for $IV_t$ and when no microstructure noise is present.

The distribution of $\xi$ differs quite substantially, the $\xi$ distributions with true parameters from panel A and C (red and blue lines) has a really heavy left tail compared to the standard normal distribution, the $\xi$ distributions with true parameter from panel B and D have higher density around the mean and a steeper right tail compared to the standard normal distribution.

The $\lambda$ distributions with true parameters from panel A and C (red and blue lines) have a heavy right tail, while the $\lambda$ distributions with true parameters from panel B and D have higher density around the mean compared to the standard normal distribution. All the $\lambda$ distributions have the highest density below zero, but the tail structure makes it a bit hard to tell whether this results in underestimation, and the earlier presented tables do not help to provide an answer.

For the third graph, the $\nu$ distributions are plotted. None of them are close to looking like a standard normal distribution, the standard normal distribution looks like a completely flat line. All the $\nu$ distributions have way higher density around their means and way steeper tails. In this graph, it seems like the variance is completely wrong.

For the fourth graph, the $H$ distributions are plotted. Out of the four graphs, it is within this graph that the distributions seems closets to standard normal. For all sets of true parameters, the distributions have negative mean and heavier tails. The distribution of $H$ with true parameters as in panel B (green line) has higher density around its mean, and vice versa for the rest of the $H$ distributions. This suggests that a general slight underestimation of $H$ using MRC as estimator for $IV_t$, which is, for the most part, consistent with the results presented in the tables, table 3.1 is an exception.

In Figure 3.2 we see the distribution of $\xi, \lambda, \nu$ and $H$ in that order, this is done with MRC as estimator for $IV_t$ with microstructure noise present.

The distributions for all the parameters for all sets of true values are surprisingly similar to the distributions seen in Figure 3.1, which emphasizes the microstructure noise robustness of the MRC estimator. Furthermore, this suggests that Theorem 13 is still valid after the inclusion of microstructure noise.

In Figure 3.3 we see the distribution of $\xi, \lambda, \nu$ and $H$ in that order, this is done with RV5 as estimator for $IV_t$ with microstructure noise present.

If we compare with the two previous figures, the main differences lie within the first and the second graph. There is not much to touch upon regarding the $\nu$ distributions, since the same problem is present as in the two previous figures. The $H$ distributions have less heavy tails compared to the previous figures, this might suggest that, if the only interest is to estimate the Hurst index. RV5 may be a better choice than MRC as the estimator for $IV_t$. However, the $\xi$ distributions are right skewed with a positive mean, and is highly suggesting an overestimation of $\xi$, which is consistent with the results presented in the tables. All the $\lambda$ distributions have negative mean with varying skewness. The general tendency suggests underestimations, this does however seem to be case dependent, when comparing with the tables.

In Figure 3.4, the distribution for the test statistic from the second approach for each of the panels is shown, where MRC and RV5 is used as estimators of $IV_t$. The first graph is with no microstructure noise, while the second and third are with microstructure noise.

We once again notice that the addition of microstructure noise, does not seem to affect the distribution of the test statistic. The distribution of the test statistic closer to the $\chi^2(4)$ distribution when MRC is the estimator for $IV_t$, however, none of the distributions seem really close to the $\chi^2(4)$. The distribution for the test statistic with true values from panel C (blue line) and MRC as estimator for $IV_t$ is the closest we get.

With the information provided by Figures 3.1, 3.2 and 3.3, it may seem that it is the distribution of $\nu$ that is ruining the distribution of the test statistic obtained via the second approach.

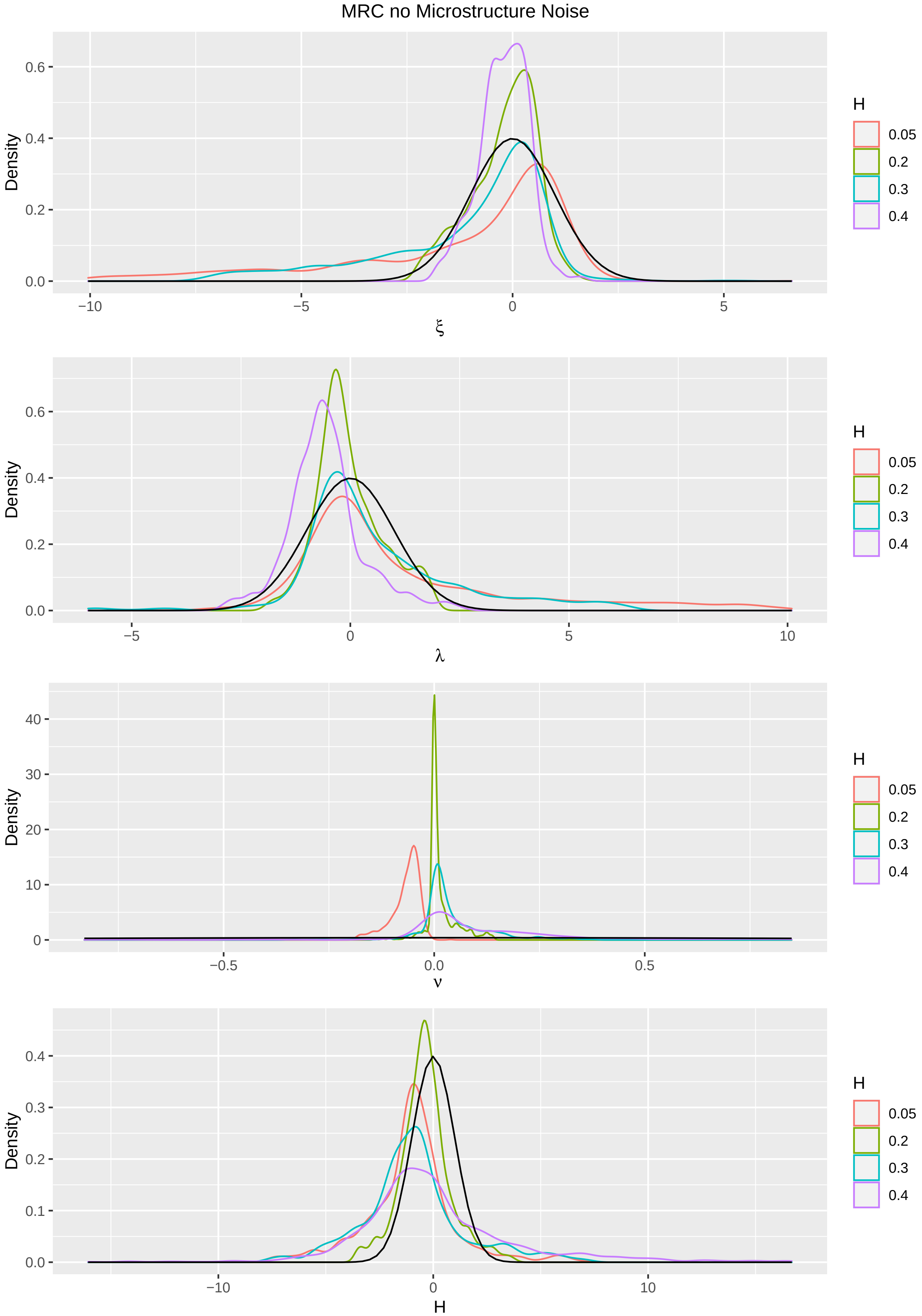


***Figure 3.1.*** Density plots for MRC without microstructure noise.

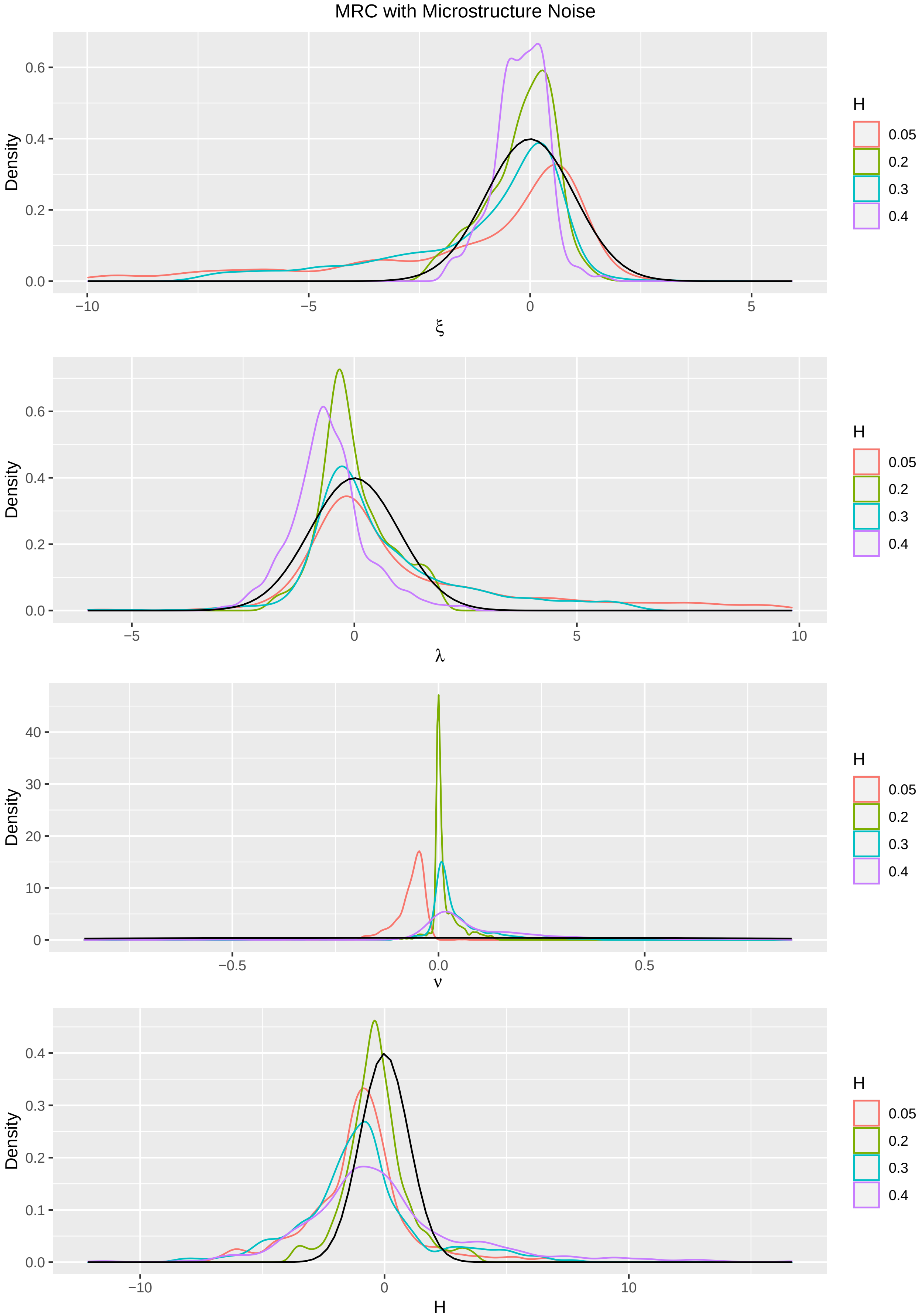


***Figure 3.2.*** Density plots for MRC with microstructure noise.

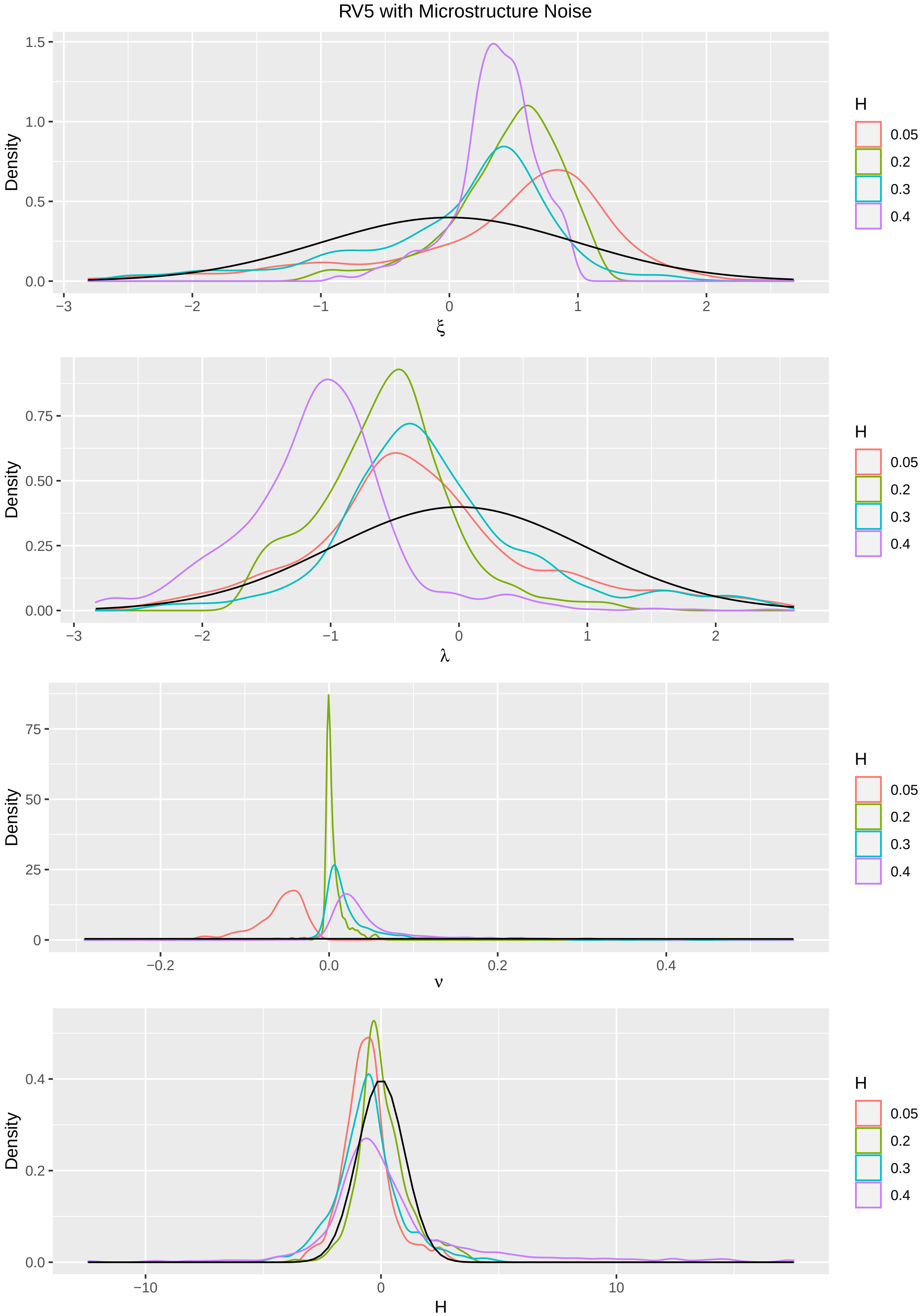


***Figure 3.3.*** Density plots for RV5 with microstructure noise.

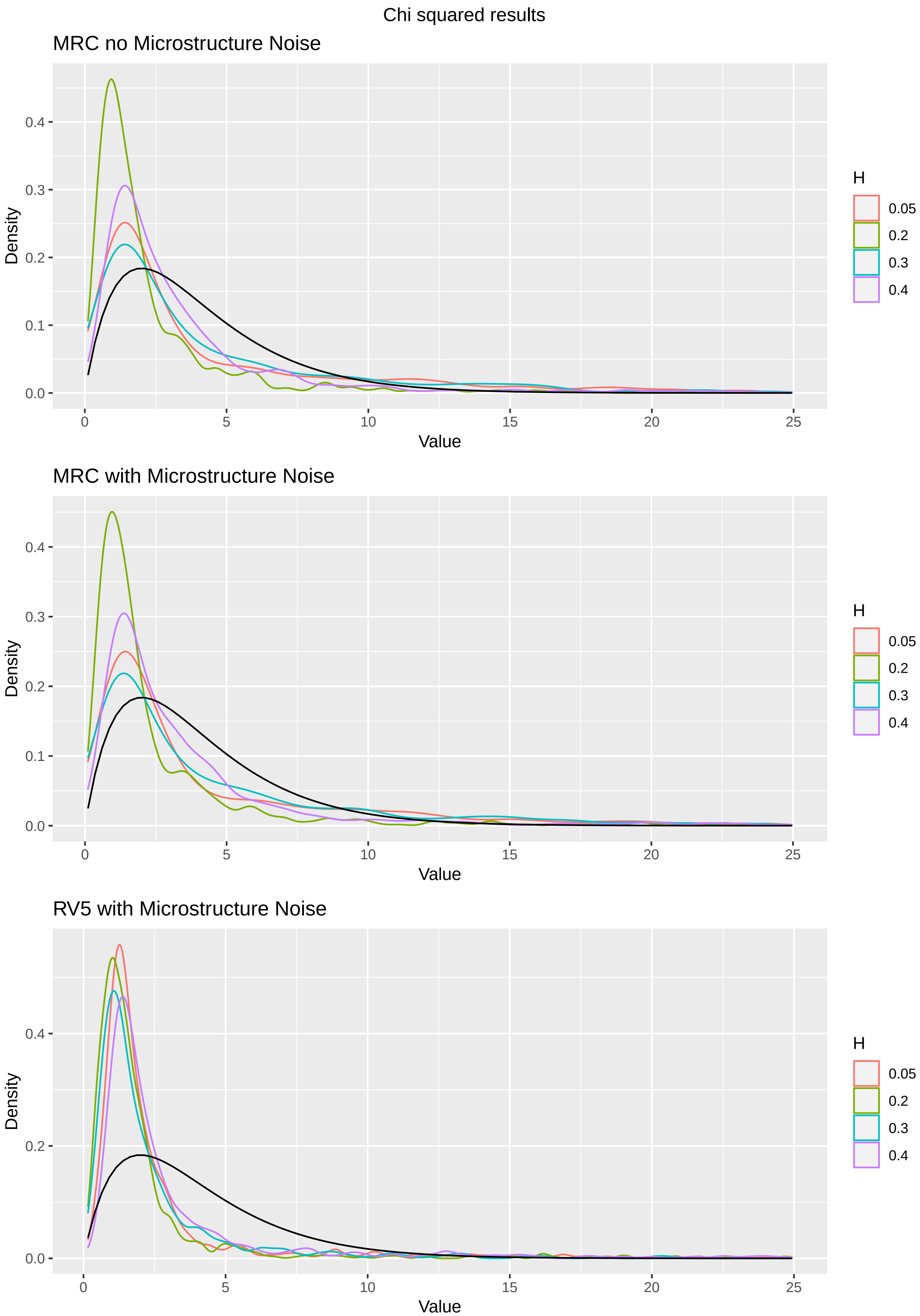


***Figure 3.4.*** Density plot for the $\chi^2$ distributions

Keep in mind that $T = 100$. This probably has an effect on distributions plotted, if $T$ was larger, the distributions might have been closer to the standard normal. Furthermore, the first approach requires 3 matrix inversions along with a Cholesky decomposition, which also might make the distributions plotted look further away from the standard normal than what the underlying true distribution actually is.

The presented graphs along with previous presented tables draw us toward the following conclusion. In the presence of microstructure noise, MRC is generally the better choice as an estimator for $IV_t$ as it overall provides the best estimates, where MRC really outshines RV and RV5 is in estimation of $\xi$. Thus, if the interest is to estimate risk, MRC is far superior. However, for solely estimating the Hurst parameter RV5 is a slightly better choice.

The GMM approach still seems to be valid in the presence of microstructure noise if a microstructure noise robust is chosen as estimator for $IV_t$. If the RV5 is chosen instead, the method might still work to estimate roughness, but the distribution presented in Theorem 13 seem incorrect.

### 3.1.2 Long Timeframe

The second part of the simulation study consists of a different setup. Namely, the setup of $T = 1000$, $n = 23400$ and 1000 replications, here we have only investigated the following set of parameters.

1. Panel A: $\xi = 0.0225$, $\lambda = 0.005$, $\nu = 1.25$ and $H = 0.05$, with results found in Table 3.5.
2. Panel B: $\xi = 0.0225$, $\lambda = 0.015$, $\nu = 0.5$ and $H = 0.2$, with results found in Table 3.6.
3. Panel C: $\xi = 0.0225$, $\lambda = 0.015$, $\nu = 0.5$ and $H = 0.3$, with results found in Table 3.7.
4. Panel D: $\xi = 0.0225$, $\lambda = 0.035$, $\nu = 0.3$ and $H = 0.4$, with results found in Table 3.8.

The increase of $T$ greatly improves the $H$ estimates for larger true values of $H$. When $T = 100$ the estimates of $H$ only varied between 0.1 and 0.2 even for larger values of true $H$. Furthermore, the $H$ estimates are way better when MRC is used as an estimator for $IV_t$ compared to RV and RV5 when the true $H$ is larger than 0.05 as seen in Table 3.6, 3.7 and in Table 3.8. Interestingly enough, microstructure noise does not seem to affect the $H$ estimation when RV is used as estimator for $IV_t$, RV as estimator, does once again overestimate $\xi$ no matter the set of true parameters. This is not the case when RV5 is the estimator for $IV_t$, as it was in scenario one. This suggests an improvement when using MRC as the estimator for $IV_t$ compared to RV and RV5.

Another observation is that the standard deviations for all parameters, with or without microstructure noise present, are greater for the results presented in Section 3.1.1, with $T = 100$ compared to the results in the following tables. This follows from the greater value of $T$, which from Theorem 11 effects the variance of the estimated values.

| Parameter | | $\xi$ | $\lambda$ | $\nu$ | $H$ |
|---|---|---|---|---|---|
| True | | 0.0225 | 0.005 | 1.25 | 0.05 |
| IV | Initial | 0.0251 (0.0098) | 0.0284 (0.0141) | 0.457 (0.0117) | 0.266 (0.0195) |
| | Estimate | 0.0236 (0.00878) | 0.0256 (0.023) | 0.659 (0.0492) | 0.168 (0.023) |
| No microstructure noise | | | | | |
| RV | Initial | 0.0264 (0.0142) | 0.0279 (0.0143) | 0.457 (0.0117) | 0.265 (0.0194) |
| | Estimate | 0.0246 (0.012) | 0.0259 (0.0289) | 0.66 (0.0557) | 0.169 (0.0326) |
| RV5 | Initial | 0.0264 (0.0141) | 0.0222 (0.0129) | 0.522 (0.0135) | 0.221 (0.0185) |
| | Estimate | 0.0238 (0.0118) | 0.0368 (0.0713) | 0.688 (0.0754) | 0.167 (0.046) |
| MRC | Initial | 0.0264 (0.0157) | 0.0262 (0.014) | 0.474 (0.0121) | 0.253 (0.0192) |
| | Estimate | 0.0245 (0.0139) | 0.0285 (0.0441) | 0.669 (0.0563) | 0.168 (0.045) |
| With microstructure noise | | | | | |
| RV | Initial | 0.189 (0.0739) | 0.0276 (0.0139) | 0.466 (0.012) | 0.259 (0.0193) |
| | Estimate | 0.177 (0.0658) | 0.0336 (0.0614) | 0.666 (0.0594) | 0.176 (0.0859) |
| RV5 | Initial | 0.0269 (0.0144) | 0.0222 (0.0129) | 0.521 (0.0134) | 0.221 (0.0185) |
| | Estimate | 0.0243 (0.0121) | 0.0361 (0.0692) | 0.687 (0.0737) | 0.168 (0.0456) |
| MRC | Initial | 0.0262 (0.014) | 0.0262 (0.014) | 0.474 (0.0121) | 0.253 (0.0192) |
| | Estimate | 0.0243 (0.0119) | 0.0289 (0.0439) | 0.668 (0.0545) | 0.169 (0.0439) |

***Table 3.5.*** Panel A. Scenario two

| Parameter | | $\xi$ | $\lambda$ | $\nu$ | $H$ |
|---|---|---|---|---|---|
| True | | 0.0225 | 0.015 | 0.5 | 0.2 |
| IV | Initial | 0.0229 (0.00339) | 0.038 (0.0117) | 0.318 (0.00804) | 0.367 (0.0203) |
| | Estimate | 0.0224 (0.00319) | 0.0181 (0.0153) | 0.527 (0.0818) | 0.189 (0.0566) |
| No microstructure noise | | | | | |
| RV | Initial | 0.0229 (0.00338) | 0.0379 (0.0117) | 0.318 (0.00801) | 0.366 (0.0203) |
| | Estimate | 0.0224 (0.00319) | 0.0183 (0.0157) | 0.526 (0.0824) | 0.19 (0.0576) |
| RV5 | Initial | 0.0229 (0.00338) | 0.0261 (0.0101) | 0.392 (0.0101) | 0.281 (0.0192) |
| | Estimate | 0.0219 (0.00314) | 0.0187 (0.014) | 0.595 (0.04) | 0.165 (0.0267) |
| MRC | Initial | 0.0227 (0.00335) | 0.0345 (0.0113) | 0.336 (0.00856) | 0.343 (0.0201) |
| | Estimate | 0.0221 (0.00316) | 0.0172 (0.0125) | 0.549 (0.0639) | 0.177 (0.0418) |
| With microstructure noise | | | | | |
| RV | Initial | 0.134 (0.0198) | 0.0377 (0.0116) | 0.319 (0.00809) | 0.365 (0.0202) |
| | Estimate | 0.131 (0.0187) | 0.0179 (0.0151) | 0.533 (0.0823) | 0.186 (0.0558) |
| RV5 | Initial | 0.0233 (0.00343) | 0.0261 (0.0101) | 0.392 (0.0101) | 0.281 (0.0193) |
| | Estimate | 0.0223 (0.00319) | 0.0187 (0.0142) | 0.596 (0.0385) | 0.165 (0.027) |
| MRC | Initial | 0.0227 (0.00336) | 0.0344 (0.0113) | 0.336 (0.00858) | 0.343 (0.0201) |
| | Estimate | 0.0221 (0.00316) | 0.0173 (0.0127) | 0.548 (0.0652) | 0.178 (0.0429) |

***Table 3.6.*** Panel B. Scenario two

| Parameter | | $\xi$ | $\lambda$ | $\nu$ | $H$ |
|---|---|---|---|---|---|
| True | | 0.0225 | 0.015 | 0.5 | 0.3 |
| IV | Initial | 0.0233 (0.00771) | 0.0331 (0.0104) | 0.362 (0.00913) | 0.437 (0.0206) |
| | Estimate | 0.0218 (0.00687) | 0.0198 (0.0295) | 0.545 (0.123) | 0.261 (0.0956) |
| No microstructure noise | | | | | |
| RV | Initial | 0.0233 (0.0077) | 0.0331 (0.0103) | 0.362 (0.00911) | 0.437 (0.0206) |
| | Estimate | 0.0218 (0.00686) | 0.019 (0.0231) | 0.544 (0.123) | 0.26 (0.092) |
| RV5 | Initial | 0.0232 (0.00761) | 0.0237 (0.00885) | 0.428 (0.011) | 0.361 (0.0201) |
| | Estimate | 0.0212 (0.00665) | 0.0132 (0.0164) | 0.631 (0.0873) | 0.207 (0.0576) |
| MRC | Initial | 0.023 (0.00757) | 0.0305 (0.00994) | 0.378 (0.00962) | 0.417 (0.0205) |
| | Estimate | 0.0215 (0.0067) | 0.018 (0.0343) | 0.571 (0.108) | 0.242 (0.0876) |
| With microstructure noise | | | | | |
| RV | Initial | 0.136 (0.0449) | 0.0329 (0.0103) | 0.364 (0.00921) | 0.435 (0.0205) |
| | Estimate | 0.126 (0.04) | 0.0471 (0.113) | 0.559 (0.127) | 0.295 (0.182) |
| RV5 | Initial | 0.0236 (0.00774) | 0.0237 (0.00886) | 0.428 (0.011) | 0.361 (0.0201) |
| | Estimate | 0.0215 (0.00677) | 0.0129 (0.0123) | 0.631 (0.0835) | 0.206 (0.0524) |
| MRC | Initial | 0.023 (0.00756) | 0.0305 (0.00994) | 0.378 (0.00962) | 0.417 (0.0205) |
| | Estimate | 0.0214 (0.00671) | 0.0181 (0.0343) | 0.57 (0.11) | 0.242 (0.0877) |

***Table 3.7.*** Panel C. Scenario two

| Parameter | | $\xi$ | $\lambda$ | $\nu$ | $H$ |
|---|---|---|---|---|---|
| True | | 0.0225 | 0.035 | 0.3 | 0.4 |
| IV | Initial | 0.0227 (0.00339) | 0.0488 (0.0108) | 0.235 (0.00582) | 0.499 (0.0208) |
| | Estimate | 0.0222 (0.00325) | 0.0416 (0.026) | 0.303 (0.035) | 0.392 (0.0745) |
| No microstructure noise | | | | | |
| RV | Initial | 0.0227 (0.00339) | 0.0487 (0.0107) | 0.236 (0.0058) | 0.499 (0.0208) |
| | Estimate | 0.0222 (0.00325) | 0.0414 (0.0264) | 0.303 (0.0344) | 0.391 (0.0736) |
| RV5 | Initial | 0.0227 (0.00337) | 0.0279 (0.00847) | 0.324 (0.00807) | 0.351 (0.0205) |
| | Estimate | 0.0216 (0.00315) | 0.0132 (0.0099) | 0.513 (0.0464) | 0.187 (0.0362) |
| MRC | Initial | 0.0225 (0.00333) | 0.0423 (0.01) | 0.257 (0.00637) | 0.456 (0.0208) |
| | Estimate | 0.0219 (0.00319) | 0.0273 (0.0165) | 0.354 (0.041) | 0.312 (0.0635) |
| With microstructure noise | | | | | |
| RV | Initial | 0.13 (0.0194) | 0.0486 (0.0107) | 0.236 (0.00583) | 0.498 (0.0207) |
| | Estimate | 0.127 (0.0186) | 0.0417 (0.0293) | 0.306 (0.0425) | 0.39 (0.0803) |
| RV5 | Initial | 0.023 (0.00342) | 0.0279 (0.0085) | 0.324 (0.00804) | 0.351 (0.0206) |
| | Estimate | 0.0219 (0.0032) | 0.0132 (0.0101) | 0.513 (0.0463) | 0.187 (0.0367) |
| MRC | Initial | 0.0225 (0.00333) | 0.0422 (0.01) | 0.257 (0.00638) | 0.456 (0.0208) |
| | Estimate | 0.0219 (0.00319) | 0.0273 (0.0167) | 0.354 (0.0407) | 0.312 (0.0634) |

***Table 3.8.*** Panel D. Scenario two

### Distribution of Estimates

For this section, we will keep it short and only include the MRC distribution for the first method. The color schemes in the following figures will refer to different sets of true values, as well as either a standard normal distribution for reference. The color scheme is as follows

- Red: Panel A.
- Green: Panel B.
- Blue: Panel C.
- Purple: Panel D.
- Black: Standard normal distribution.

In Figure 3.5 and 3.6 we see the parameter distribution of parameters when MRC is used as the estimator for $IV_t$ when no microstructure noise is present and when microstructure noise is present respectively. In general, it seems like the distributions somehow have diverged further from the standard normal distribution. The distributions of $\lambda$ look like they could be normal, but with a variance different from one, this does not seem to be the case for the rest of the distributions. The distribution of $H$ with true parameters from panel A looks like it is negatively biased, which is clearly not the case when looking at Table 3.5, this could indicate issues related to the Cholesky decomposition, which includes the inversion of $L$, the estimation of $\Sigma_{\mathbb{IV}}$, the estimation of $J$ and the inversion of $(J^\top \Sigma_{\mathbb{IV}}^{-1} J)$.

It is hard to pin down exactly why the divergence from the normal distribution occurs. It could be a numerical problem due to all the inversions, it could be related to issues with the optimization procedure, it could be related to estimation of some of the matrices, it could be related to the finiteness of the simulation study.

The distributions for when microstructure noise is not present are again similar to the distributions for when microstructure noise is present. Which indicates the same as the plots in Section 3.1.1 did. Namely, that Theorem 13 is still valid in the presence of microstructure noise when using a microstructure robust estimator.

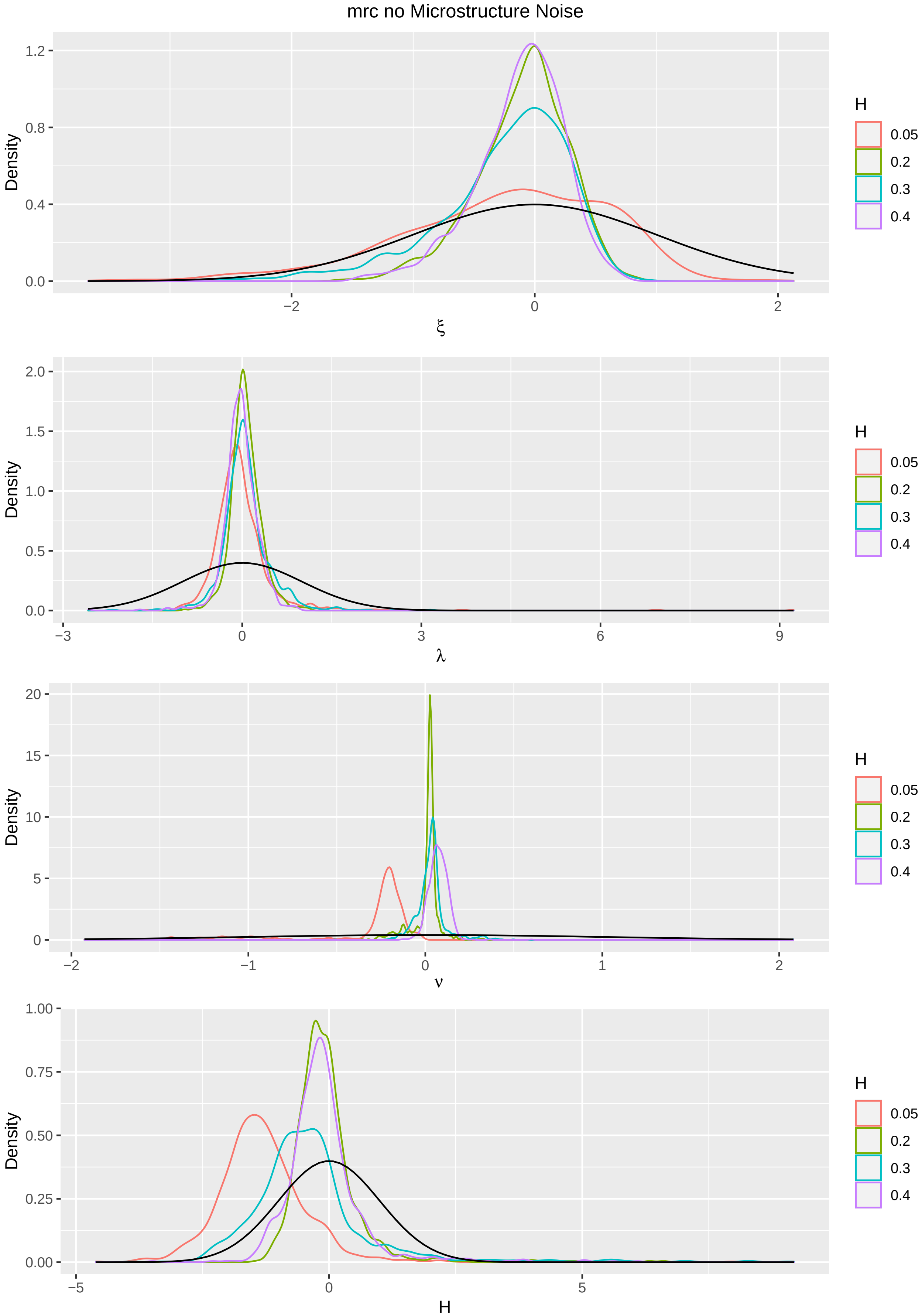


***Figure 3.5.*** Densities MRC without microstructure noise

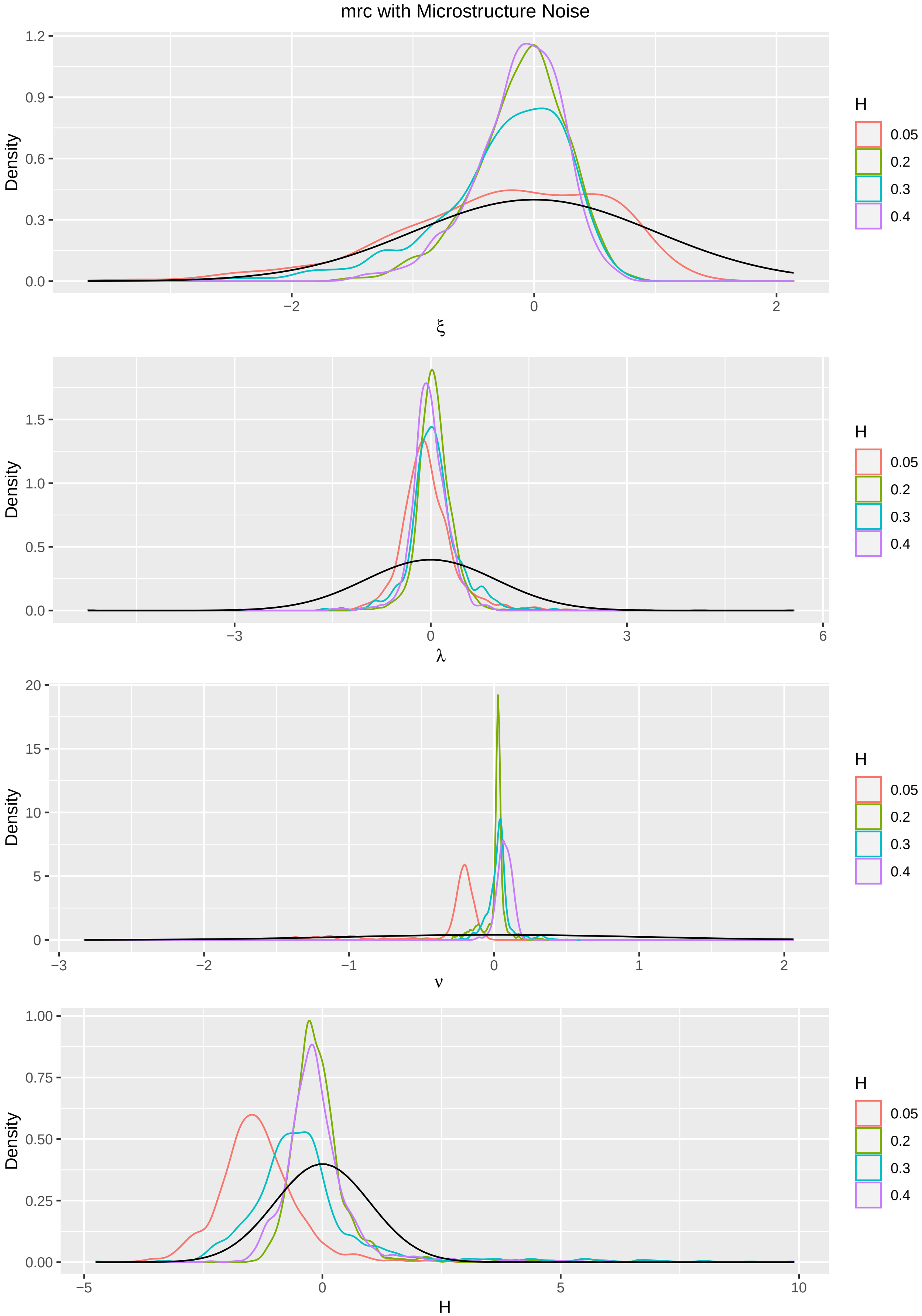


***Figure 3.6.*** Densities MRC with microstructure noise

Chapter 4

# Application

In the empirical application, we would like to investigate S&P500. We would like to assume that the underlying unobserved log-price process is generated by (2.1) and that the observed price is a noise version as in (2.14). We are going to assumes that the volatility process is driven by a fractional Ornstein-Uhlenbeck process. We would like to estimate the parameters, here are the $\xi$ and $H$ of special interest. Before we get started, some data cleaning is needed. The data we will be using is trade data from 1999 to 2009, and the cleaning process we use is the one described in Section 3 of [Barndorff-Nielsen et al., 2009]. In summary, the data is filtered to include only trades from one exchange, NYSE in this application, and outlier prices are removed using a rolling centered median approach.

**Introduction to Data**

In the first graph of Figure 4.1 is the close price primo 1999 to ultimo 2009 plotted. In the second graph of figure 4.1 is the MRC and RV5 estimates of $IV_t$ plotted from primo 1999 to ultimo 2009. The average number of observations per day is 9058, while the largest number of observation for a day is 22809 and the minimum number of observation for a day is 213. Since the data is primo 1999 to ultimo 2009 the observations per day is steadily increasing as time progresses which can be seen In Figure 4.2. This emphasizes that importance of a setting that utilizes high frequency. In the period from the 8th of February 2007 to the 23rd of February 2007, the number of observations per day suddenly drops from about 10000 to about 500. It is not clear why this occurs, investigating the price during this period does not help to provide an answer. As seen in Figure 4.3, there is nothing too suspicious to note. CNN reports that the 27th of February 2007 was the worst day in 4 years for S&P500 with a decrease of 3.5 percent [https://edition.cnn.com/business, 2007] , according to Wikipedia was a trading room at 30 Broad Street closed in February 2007 [en.wikipedia.org, 2022], which in itself does explain the low trading frequencies, but it may be part of the explanation. The period from 2007-02-08 to 2007-02-23 will be removed from the data due to the low trading frequency.

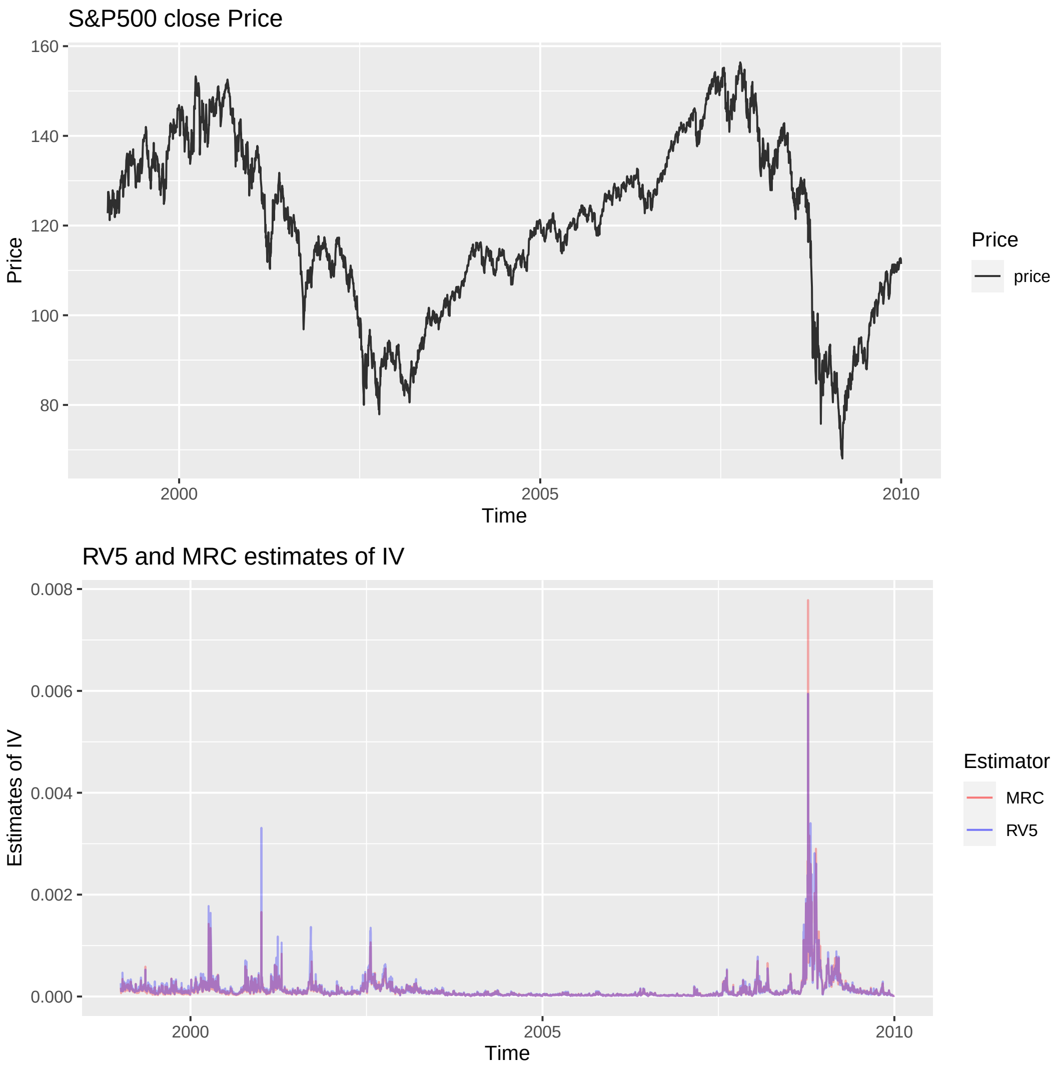


***Figure 4.1.*** First graph: The close Price of S&P500 from primo 1999 to ulitmo 2009. Second graph: $IV_t$ estimates for s&P500 from primo 1999 to ultimo 2009.

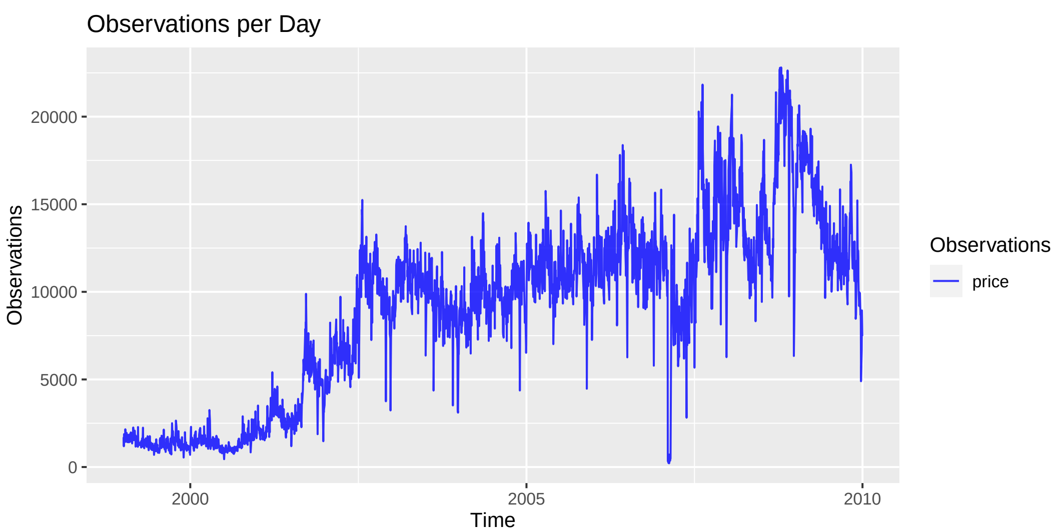


***Figure 4.2.*** How often S&P500 is traded during a day.

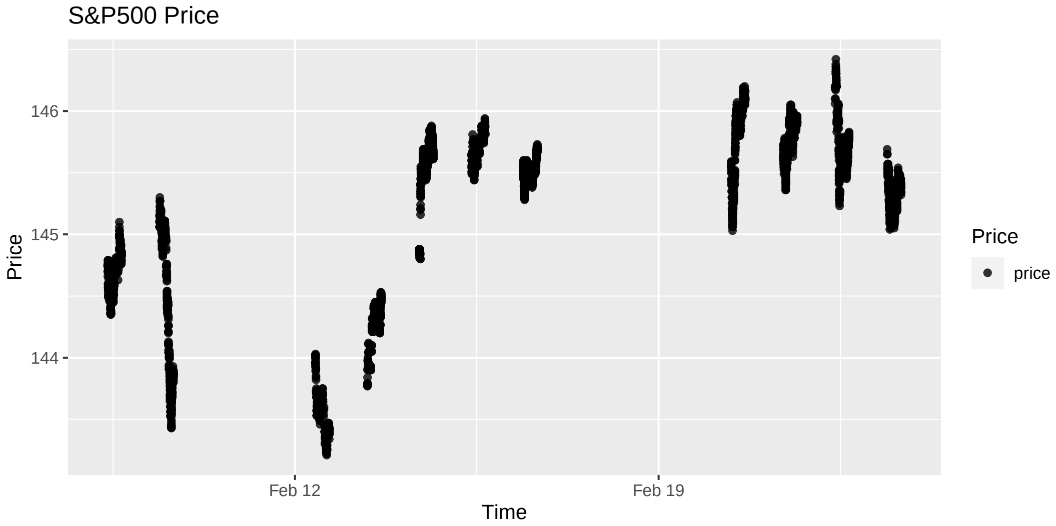


***Figure 4.3.*** S&P500 Price from 2007-02-08 to 2007-02-23.

### Parameter Estimation

In the Table 4.1 we see the initial guesses along with the estimated parameters for the assumed underlying driver of the volatility model. No matter the use of the estimator, we achieve quite similar estimates for the Hurst index, they differ at the 3rd digit. If we are to compare with other empirical findings, in [Gatheral et al., 2018] they estimated the Hurst index, with a different method, for S&P 500 to 0.142 for the period January 2000 to March 2014, which is relatively close to hour estimates. In [Bolko et al., 2022] they estimated the Hurst index for S & P500 to 0.043 for the period January 2000 to July 2019, this results differs a bit from our results. However, we have generally struggled with estimations of the Hurst index, when it is below 0.1. But nevertheless, we draw the same conclusion as many before us, for S&P 500, volatility is rough.

We once again see that, when RV is used as estimator for $IV_t$, the estimate of $\xi$ is significantly higher, than when RV5 or MRC is the estimator for $IV_t$.

From the findings through the simulation study, we generally trust that the estimated provided when MRC is used as estimator for $IV_t$ is the most reliable.

| Parameter | | $\xi$ | $\lambda$ | $\nu$ | $H$ |
|---|---|---|---|---|---|
| RV | Initial | 0.00038 | 0.000073 | 0.4537 | 0.1347 |
| | Estimate | 0.000342 | 0.00021 | 0.4537 | 0.13471 |
| RV5 | Initial | 0.00014 | 0.000802 | 0.53573 | 0.14695 |
| | Estimate | 0.0001158 | 0.000266 | 0.53454 | 0.11924 |
| MRC | Initial | 0.00013 | 0.0018 | 0.48762 | 0.1749 |
| | Estimate | 0.0001094 | 0.00019 | 0.47666 | 0.12814 |

***Table 4.1.*** S&P 500 Parameter estimation

Chapter 5

# Conclusion

## 5.1 Discussion

Regarding the validation of generalized method of moments to estimate parameters in the process driving the volatility process, there are a number of decisions made, that could have been made differently.

We did not decide to include a moment correction as in [Bolko et al., 2022], even though the moment correction made is based on the $IV_t$ observed, being described as a noisy proxy which is not the case in the double asymptotic setting i.e. the moment correction term vanishes. However, we are still operating within a finite setup and [Bolko et al., 2022] states that, one might as well include the moment correction term, since nothing is lost by adding it. The inclusion of the moment correction term, could potentially have improved the estimation.

Our optimization procedure generally struggles in estimation of $H$ for small values of the Hurst index. The optimization algorithms used in this project have been either Nelder-Mead with tolerance $10^{-6}$ or BFGS with tolerance $10^{-8}$. In [Bolko et al., 2022], they used a gradient-based non-linear least squares Matlab function called lsqnonlin with the algorithm trust-region reflective and a tolerance level of $10^{-6}$. Our implementation has been in R, and we did try the equivalent algorithm, which provided us with worse results. Even though we did not find any algorithms that provided us with better results, there might be algorithms better suited for the specific problem at hand.

In the project, we have only been concern about one end of the spectrum of fractional volatility models. The optimization procedure would be able to estimate $H > 0.5$ as shown in [Bolko et al., 2022], however the Theorem 13, on the asymptotic distribution of the parameters, ceases to hold. This focus is primarily taken due to existing literature on the topic suggesting that volatility is rough, which agrees with the empirical findings presented in this project.

In the investigation of the distribution of the parameters, we primarily relied on the test statistic $L^{-\top}(\sqrt{T}(\widetilde{\theta}_{n,T} - \theta_0))$. Which, as mentioned, includes 3 matrix inversions and a Cholesky decomposition. A different approach for single parameter investigation could be to simply pick the scaled parameter estimates minus the true values and divide those by the corresponding diagonal entries in $(J^\top \Sigma_{\mathbb{IV}}^{-1} J)^{-1}$. This approach would have been more numerical robust, but might be dependent on the covariance structure between the parameters in finite samples.

## 5.2 Conclusion

Related to the investigation of the parameter distribution is the validation of Theorem 13 in the presence of microstructure noise. Even though, the parameter distribution presented when MRC was used as estimator for $IV_t$ generally diverged from the standard normal distribution. The addition of microstructure noise barely changed anything about the distribution. Which one may argue points towards the Theorem 13 still being valid in the presence of microstructure noise, at least with a microstructure robust estimator for $IV_t$.

The empirical analysis agrees with existing literature on volatility being rough. When MRC was used as estimator for $IV_t$ we estimated the Hurst index of S&P 500 to 0.128 which is on par with [Gatheral et al., 2018] who got a Hurst index of 0.142 but further away from [Bolko et al., 2022] with a Hurst index of 0.043.

# Bibliography


Fischer Black and Myron Scholes. The pricing of options and corporate liabilities. *Journal of Political Economy*, 81(3):637–654, 1973. ISSN 00223808, 1537534X. URL http://www.jstor.org/stable/1831029.

Bruno Dupire, The Black–scholes Model (see Black, and Gives Options. Pricing with a smile. *Risk Magazine*, pages 18–20, 1994.

Jim Gatheral, Thibault Jaisson, and Mathieu Rosenbaum. Volatility is rough. *Quantitative Finance*, 18(6): 933–949, 2018. doi: 10.1080/14697688.2017.1393551. URL https://doi.org/10.1080/14697688.2017.1393551.

Masaaki Fukasawa. Asymptotic analysis for stochastic volatility: martingale expansion. *Finance and Stochastics*, 15:635–654, 2011.

Anine Eg Bolko. *Modelling and Forecasting Fractional Volatility*. PhD thesis, January 2021. Termination date: 25-01-2021.

Kim Christensen, Silja Kinnebrock, and Mark Podolskij. Pre-averaging estimators of the ex-post covariance matrix in noisy diffusion models with non-synchronous data. *Journal of Econometrics*, 159(1):116–133, 2010. ISSN 0304-4076. doi: https://doi.org/10.1016/j.jeconom.2010.05.001. URL https://www.sciencedirect.com/science/article/pii/S0304407610001260.

Anine E. Bolko, Kim Christensen, Mikko S. Pakkanen, and Bezirgen Veliyev. A gmm approach to estimate the roughness of stochastic volatility, 2022. URL https://arxiv.org/abs/2010.04610.

Patrick Cheridito, Hideyuki Kawaguchi, and Makoto Maejima. Fractional Ornstein-Uhlenbeck processes. *Electronic Journal of Probability*, 8(none):1 – 14, 2003. doi: 10.1214/EJP.v8-125. URL https://doi.org/10.1214/EJP.v8-125.

Terhi Kaarakka and Paavo Salminen. On fractional ornstein-uhlenbeck process. *Communications on Stochastic Analysis*, 5(1):121–133, 2011. ISSN 0973-9599.

Ole E. Barndorff-Nielsen and Andreas Basse-O'Connor. Quasi ornstein–uhlenbeck processes. *Bernoulli*, 17 (3), aug 2011. doi: 10.3150/10-bej311. URL https://doi.org/10.3150%2F10-bej311.

Josselin Garnier and Knut Sølna. Option pricing under fast-varying and rough stochastic volatility. *Annals of Finance*, 14:489–516, 2018.

Asbjørn Bach Andreassen and Rasmus Dam. Portfolio allocation with value at risk using intraday high frequency prices in the presence of microstructure noise. 2021. URL https://projekter.aau.dk/projekter/da/studentthesis/portfolio-allocation-with-value-at-risk-using-intraday-high-frequency-prices-in-the-presence-of.html.

Søren Asmussen and Peter W. Glynn. *Gaussian Processes*, pages 306–324. Springer New York, New York, NY, 2007. ISBN 978-0-387-69033-9. doi: 10.1007/978-0-387-69033-9_11. URL https://doi.org/10.1007/978-0-387-69033-9_11.

Federico M. Bandi and Jeffrey R. Russell. Separating microstructure noise from volatility. *Journal of Financial Economics*, 79(3):655–692, 2006. ISSN 0304-405X. doi: https://doi.org/10.1016/j.jfineco.2005.01.005. URL `https://www.sciencedirect.com/science/article/pii/S0304405X05001534`.

O. E. Barndorff-Nielsen, P. Reinhard Hansen, A. Lunde, and N. Shephard. Realized kernels in practice: trades and quotes. *The Econometrics Journal*, 12(3):C1–C32, 2009. ISSN 13684221, 1368423X. URL `http://www.jstor.org/stable/23116045`.

https://edition.cnn.com/business. Brutal day on Wall Street. 2007. URL `https://money.cnn.com/2007/02/27/markets/markets_0405/index.htm`.

en.wikipedia.org. New York Stock Exchange. 2022. URL `https://en.wikipedia.org/wiki/New_York_Stock_Exchange`.